STRUCTURE FUNCTION STUDIES OF THE NDHD4 PROTEIN OF THE CO_2 UPTAKE MECHANISM IN *SYNECHOCOCCUS ELONGATUS sp.* PCC 7942

By

CLARK K. JETT

Bachelor of Science in Biology

University of Wyoming

Laramie, WY, USA

2019

Submitted to the Faculty of the

Graduate College of the

Oklahoma State University

in partial fulfillment of

the requirements for

the Degree of

MASTER OF SCIENCE

July, 2022

STRUCTURE FUNCTION STUDIES OF

THE NDHD4 PROTEIN OF THE CO_2 UPTAKE MECHANISM

IN *SYNECHOCOCCUS ELONGATUS* sp. PCC 7942

Thesis Approved:

Robert L. Burnap

Thesis Advisor

Wouter Hoff

Randy Morgenstein

Noha H. Youseff

ACKNOWLEDGEMENTS

I would like to thank my advisor Dr. Robert L. Burnap for the support and guidance during my time in his lab. I would like to thank my committee members for kindly volunteering their time and energy to help with my academic and scientific development. I would also like to thank Minquan Zhang for his help with protein expression. I am extremely grateful for my current lab member Ross Walker. He has given me a great deal of assistance throughout my thesis. In addition, I am very grateful for the tireless efforts of Dr. Anton P. Avromov for his contributions in constructing and implementing the CRISPR gene deletion system. I am also thankful for his friendship and guidance during our time in the lab together. Also, I would like to thank Dr. Neil T. Miller for teaching me various scientific procedures/protocols. I appreciate the help of Dr. Lei Lei of the DNA/Protein Resource Facility at Oklahoma State University for her fantastic DNA sequencing. This work was made possible through the financial support of the U.S. Department of Energy (DOE), Office of Science, Basic Energy Sciences, grant no. DE-FG02-08ER15968

I would like to thank my parents, my brother Robert, and the rest of my family, for their unwavering support during my time here. My brother has sacrificed a great deal of his time and money to make frequent visits, for which I am grateful. I would also like to thank Rosalie Dohmen for all her support during my time here. She was always there for me during all the

trials and tribulations of graduate school. Finally, I would like to thank my friends back home and all the friends I have made here for their continuous support.

Name: CLARK JETT

Date of Degree: JULY, 2022

Title of Study: STRUCTURE FUNCTION STUDIES OF THE NDHD4 PROTEIN OF THE CO_2 UPTAKE MECHANISM IN *SYNECHOCOCCUS ELONGATUS* sp. PCC 7942

Major Field: MICROBIOLOGY, CELL AND MOLECULAR BIOLOGY

Abstract: To overcome the poor kinetic efficiency of Rubisco, cyanobacteria have evolved a CO_2-concentrating mechanism (CCM) that maintains high carbonation levels in the cytoplasm. The cyanobacterial CCM utilizes a modified NADH dehydrogenase oxidoreductases (NDH-$1_{3,4}$) to hydrate CO_2 to bicarbonate (HCO_3^-) using photosynthetic redox energy. The energetic coupling effectively captures the inorganic carbon (C_i) in the cell in a form that is efficiently used within the carboxysome for fixation into sugars. The coupling mechanism by NDH-$1_{3,4}$, along with the rest of the CCM, acts as a supercharger for CO_2, saturating Rubisco's active sites and avoiding photorespiration.

Here, I test the hypothesis that proton-pumping by the antiporter-like NdhD4 subunit of the NDH-1_4 complex is essential for coupling of CO_2 hydration to NDH-1 electron transfer. Structural modeling shows that amino acids involved in proton pumping in other species (e.g., *E. coli*) are conserved in NdhD4. The overall carbonic anhydrase (CA)-like reaction in the Zn-containing CupB subunit is somehow coupled to an unknown energy source to drive the reaction far-from-equilibrium in favor of bicarbonate production. By analogy with known carbonic anhydrases (CAs) and characteristics of CupB mutants, we hypothesize that the NdhD4 protein functions to trap and remove protons produced in the CO_2- hydration reaction by pumping them across to the luminal side of the membrane away from the anhydrase active site and avoiding the back-reaction and driving the reaction in favor of HCO_3^- production. To probe the NdhD4 subunit's role in CO_2 hydration, I identified and mutated several residues that likely effect the proton trapping and translocating ability of the subunit. When mutated, these residues alter the photosynthetic ability of the cell, indicating that they are critical for optimal proton translocation and therefore CO_2 hydrating.

TABLE OF CONTENTS

Chapter

Page

Chapter

Page

LIST OF TABLES

Table

Page

LIST OF FIGURES

Figure

Page

CHAPTER I
INTRODUCTION/LITERATURE SURVEY

At the beginning of earth's formation, the atmosphere surrounding the planet was likely comprised of CO_2, water vapor, and particulate matter. In addition, the earth's atmosphere was essentially devoid of oxygen, especially to the extent as seen currently. These were the conditions 4.5 billion years ago (bya)(Robert E. Blankenship, 2010). It was then, not until around 3.8 bya, that the first single celled organisms are thought to have evolved. That is a gap of around 700 million years from the hypothesized formation of our terrestrial planet to the first cellular life. This timeline is not surprising considering the harsh environments of early earth. However around 2.4 bya, there is evidence that the composition of the atmosphere changed significantly, featuring a much higher portion of molecular oxygen (O_2). This event was a major turning point regarding the evolutionary rate of life on earth. The cause of this rapid increase in oxygen was a direct result of the evolutionary invention of oxygenic photosynthesis, likely from early cyanobacteria. Oxygen served to convert strong greenhouse agents, such as methane, into carbon dioxide and water, allowing the earth to cool to a more biologically friendly temperature. In addition, oxygen is a relatively high energy molecule when utilized for the full oxidation of substates via respriation, promoting more rapid biodiversification by providing ample metabolic energy.

1.2 Light-Dependent Reactions

Oxygenic photosynthesis is the biochemical process by which photoautotrophic organisms, including plants, algae, and cyanobacteria use light to create six carbon sugars that can be used to create complex carbohydrates (i.e. biomass) from inorganic carbon and water (R.E. Blankenship, 2021). In this process, molecular oxygen is produced as a byproduct/waste product. Moreover, the energy and reducing power of photosynthesis also enables the

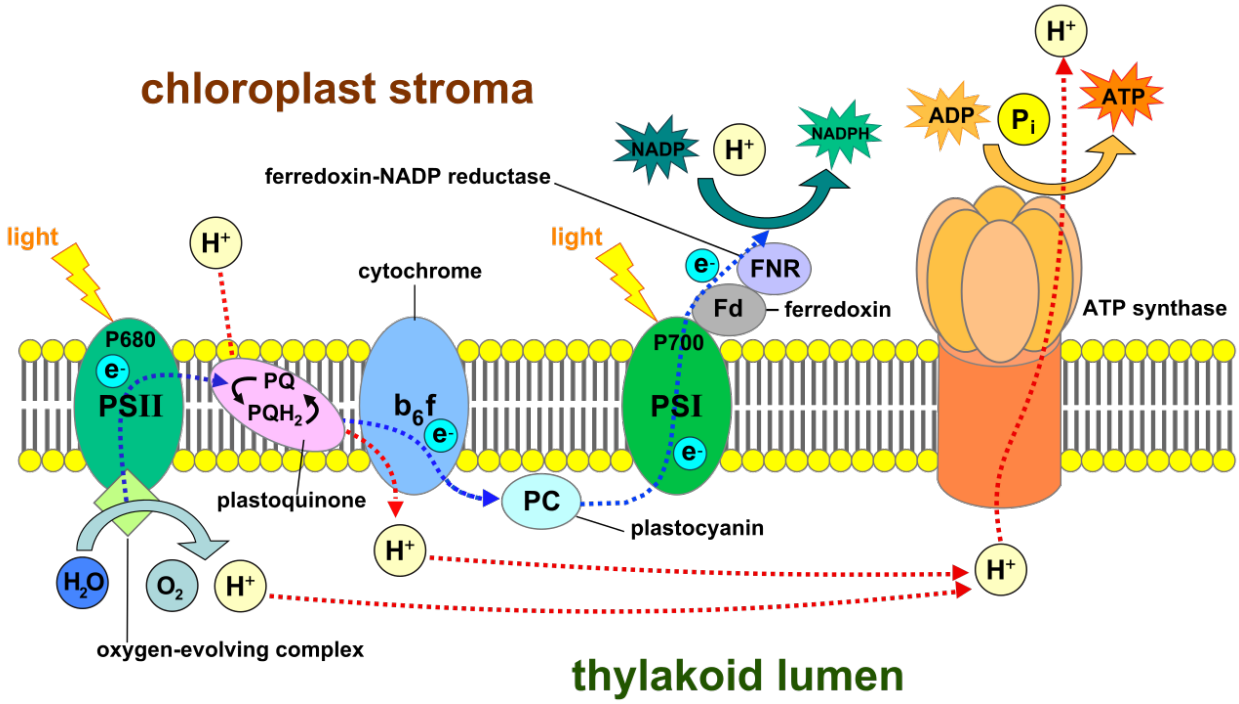

Figure 1. The photosynthetic electron transport chain (light dependent reactions) creates reducing paower in the form of NADPH as well a high energy ATP. This is done from photochemical potential energy produced in chlorophyll molecules in PSII and PSI as well as water splitting in PSII.

assimilation of other inorganic nutrients such as nitrogen to provide the basic substrates of metabolism. The process of photosynthesis is often divided into two distinct steps, occurring simultaneously. These two steps are known as the light-independent reactions and the light-dependent reactions. As seen in figure 1, the light dependent reactions are a series of processes by which light energy and water are used to create high energy ATP molecules and reducing

power in the form of NADPH. Located in the thylakoid membrane, molecules of chlorophyll (Chl) are used to absorb photons of light. Chlorophyll molecules consist of an aromatic porphyrin ring coordinating a magnesium atom(R.E. Blankenship, 2021). These molecules are arranged in large, organized groups, along with other specialized pigments, to form light harvesting antennae and photosystems. The photosystems function to receive excitation energy from photoexcited antennae as well as to directly absorb light by chlorophylls within the photosystem structrure. This energy is transferred to a special pair of Chl molecules at the so-called photochemical reaction center of the photosystem (Golbeck, 2004; Nelson & Yocum, 2006). Once the energy is effectively transferred to the special pair Chl, its electron becomes excited and charge separation occurs across the Chl and other cofactors of the reaction center (RC) (Golbeck, 2004). The photoexcited electron leaves the electronic orbital of the special pair Chl and is transferred to a nearby electron acceptor molecule, retaining much of the excitation energy in the form of the redox energy gained by the electron acceptor. Because the special pair Chl donates its energized electron, it is referred to as the primary donor of the RC, whereas the initial electron acceptor is referred to as the primary electron acceptor. In the light-dependent reactions of oxygenic photosynthesis, there are two different photosystems, photosystem I (PSI) and photosystem II (PSII). These two photosystems are rather similar in overall structure of the charge separation part of the RC, but differ in their special pair absorption and in the nature of the primary and secondary electron acceptors. The special pair of PSII undergoes photobleaching at 680 nm upon photooxidation (the process of losing an electron to the nearby primary electron acceptor), while the PSI special pair photobleaches at 700nm. PSI and PSII also differ in the cofactors involved in receiving and donating their electrons from their

corresponding primary donors. PSII receives its electrons through the oxidation of water and sequentially donates its excited electrons to the plastoquinone (PQ) pool, which is a pool of phastoquinone molecules dissolved in the thylakoid membrane lipid bilayer. During this process, energy that was harvested by the phycobilisome and/or the reaction centers, is used to energize electrons obtained by the oxidation of water, and the resultant energized electrons are donated to the PQ pool (Nelson & Yocum, 2006). Thus, PSII can be described as a water-plastoquinone oxidoreductase. However, some energy from this reaction dissipates as florescence or heat. This prevents the reaction from occurring in reverse, thus keeping it energized in a unilateral direction. Once transferred, the special pair returns to its ground state and the electron supply is replenished through the oxidation of another water molecule. Meanwhile, a similar process is happening in PSI. The difference being that PSI receives its electrons from the PQ pool, via the cytochrome b_6/f complex and then plastocyanin, which comprises the intersystem electron transport chain (Figure 1)(Mi, Endo, Schreiber, Ogawa, & Asada, 1992; Mullineaux, 2014). Electrons from plastocyanin are energized by charge separation in PSI, which donates to ferredoxin which has a very negative midpoint potential capable of then transferring elections to $NADP^+$ via ferredoxin $NADP^+$ reductase (FNR). Thus, the overall process of the light-dependent reactions uses two photosystems working in series to drive electrons from water to NADPH (R.E. Blankenship, 2021; Mullineaux, 2014). Additionally, the reduced ferredoxin is used in many other anabolic processes including nutrient uptake reactions such as the reduction of nitrate to ammonia for the production of amino acids.

In short, there are two main products produced in the light-dependent reactions. These products are reducing power in the form of NADPH and the high energy molecule ATP. These

products are then used in the light-independent reactions, also known as the Calvin-Benson-Bassham (CBB) Cycle.

1.3 Light-Independent Reactions

To successfully describe the CBB cycle, we first need to consider the main substrates CO_2 and ribulose 1,5-bisphosphate (RuBP), as well their anabolic enzyme, ribulose 1,5-bisphosphate carboxylase/oxygenase (RuBisCO), which joins them together. The first step in the CBB cycle is the carboxylation of the the five carbon ribulose 1,5 bisphosphate to form an unstable six-carbon intermediate, 3-keto-2-carboxyarabinitol-1,5-bisphosphate, which immediately is converted into two molecules of the three carbon 3-photophoglyceric acid (3-PGA). The 3-PGA can then be energized and reduced by the products produced in the light dependent reactions, ATP and NADPH, respectively. In doing so, six molecules of glyceraldehyde 3-phosphate (G3P) are produced for every six molecules of 3-PGA, ATP, and NADPH consumed. Only one of these six molecules of G3P then goes towards gluconeogenesis to synthesize six carbon sugars. The remaining 5 molecules of G3P are promptly recycled back in the CBB cycle to regenerate RuBP, using more ATP in the process. This allows the process to start over again, provided there is an adequate presence of CO_2 (Tabita, Satagopan, Hanson, Kreel, & Scott, 2008).

While the mechanism of the CBB cycle initially appears straightforward, it is complicated thanks to the enzyme kinetics of the main enzyme in the cycle, RuBisCO. RuBisCO is a notorious enzyme as it is the easily the most abundant enzyme on earth, yet it is extremely inefficient at capturing and processing CO_2. This is evident by comparing its enzyme kinetics to many common enzymes, as discussed below.

1.4 RuBisCO

To evaluate the effectiveness of RuBisCO, two main metrics are analyzed, the Michaelis constant (K_m) and the turnover time. The K_m value, of any reaction, describes the concentration of the reaction substrates at half of the maximum enzymatic rate. Furthermore, the turnover rate is simply the amount of time it takes the enzyme to turn products into reactants. RuBisCO has a K_m value of around 100 µM and a turnover time of around 100 ms (Badger, 1980). For comparison, the glycolytic enzyme hexokinase, has a K_m value of 6mM and a turnover rate of around 2 ms (Wilson, 2003).

The discrepancy in enzyme kinetics between these two extremely common enzymes can likely be attributed to two different factors. First, CO_2 is intrinsically difficult to bind into an active site on RuBisCO versus the substrate binding in hexokinase, which involves multiple hydrogen bonding and other molecular interactions. Additionally, CO_2 is in constant competition for the active site of RuBisCO with molecular oxygen, which further compounds the poor kinetic characteristics of the enzyme. If the active site of RuBisCO is bound by CO_2 and the transient six carbon intermediate is formed, then the CBB cycle can proceed. However, if the active site is bound by O_2, then a process known as photorespiration is initiated. When considering optimal functionality for carbon fixation and photosynthesis as a whole, the products of photorespiration (2-phosphoglycolate and 3-phosphoglycerate) are essentially a waste of chemical potential energy and reductants. All in, the competitive nature of products to occupy Rubisco's active site contributes to its poor kinetics. In addition, CO_2 being a small, nonpolar substrate molecule, it can passively diffuse in and out of the cell membranes. If concentrations of CO_2 are low, it will be difficult for RuBisCO to proceed in an optimal fashion and the

competing wasteful photorespiratory reaction occurs instead. All of this can be attributed to the inability of the cell to effectively sequester enough substrate around the active site.

Currently on earth there are three main groups of oxygenic photosynthetic organisms that are actively contributing to the carbon fixation and oxygen production on earth. These groups of organisms are terrestrial and aquatic plants, algae, and cyanobacteria. Of all the oxygen cycled here on earth, only about 25% of it comes from terrestrial plants, meaning the remaining 75% comes from aquatic organisms. That being said, it is estimated that the majority (~66%) of oxygen produced by marine organisms, comes from photosynthetic microorganisms, such as cyanobacteria (R.E. Blankenship, 2021). In addition, to producing a large amount of the earths oxygen, cyanobacteria also serve as a fixer of atmospheric C_i. CO_2, the most prominent example of C_i, is one of the most prevalent greenhouses gasses in the environment due to its ever-increasing abundance. CO_2 uptake and fixation is not unique to cyanobacteria as all photosynthetic organism perform CO_2 uptake and fixation. However, cyanobacteria have evolved an extremely unique way of concentrating C_i in the cell. This process is known as the Carbon Concentrating Mechanism (CCM) and features a multifaceted approach to carbonating the cells cytosol.

1.5 Carbon Concentrating Mechanism (CCM)

The CCM helps cyanobacteria overcome Rubisco's kinetic shortcomings, allowing the CBB cycle to proceed more efficiently and thus allowing photosynthesis and the production of biomass and oxygen to proceed at greater clip (Burnap, Hagemann, & Kaplan, 2015; Price, 2011; Price, Badger, Woodger, & Long, 2008).

As shown in Figure 2, the cyanobacterial CCM uses three main sub-systems to carbonate the cell (Long, Rae, Rolland, Förster, & Price, 2016). The first and most obvious, is the passive diffusion of CO_2 into the cell and to the actives sites of the population of Rubisco molecules in the cell. If the cell is present in an environment that is saturated with CO_2, then passive diffusion alone can adequately supply the demand for inorganic carbon. However, this is rarely

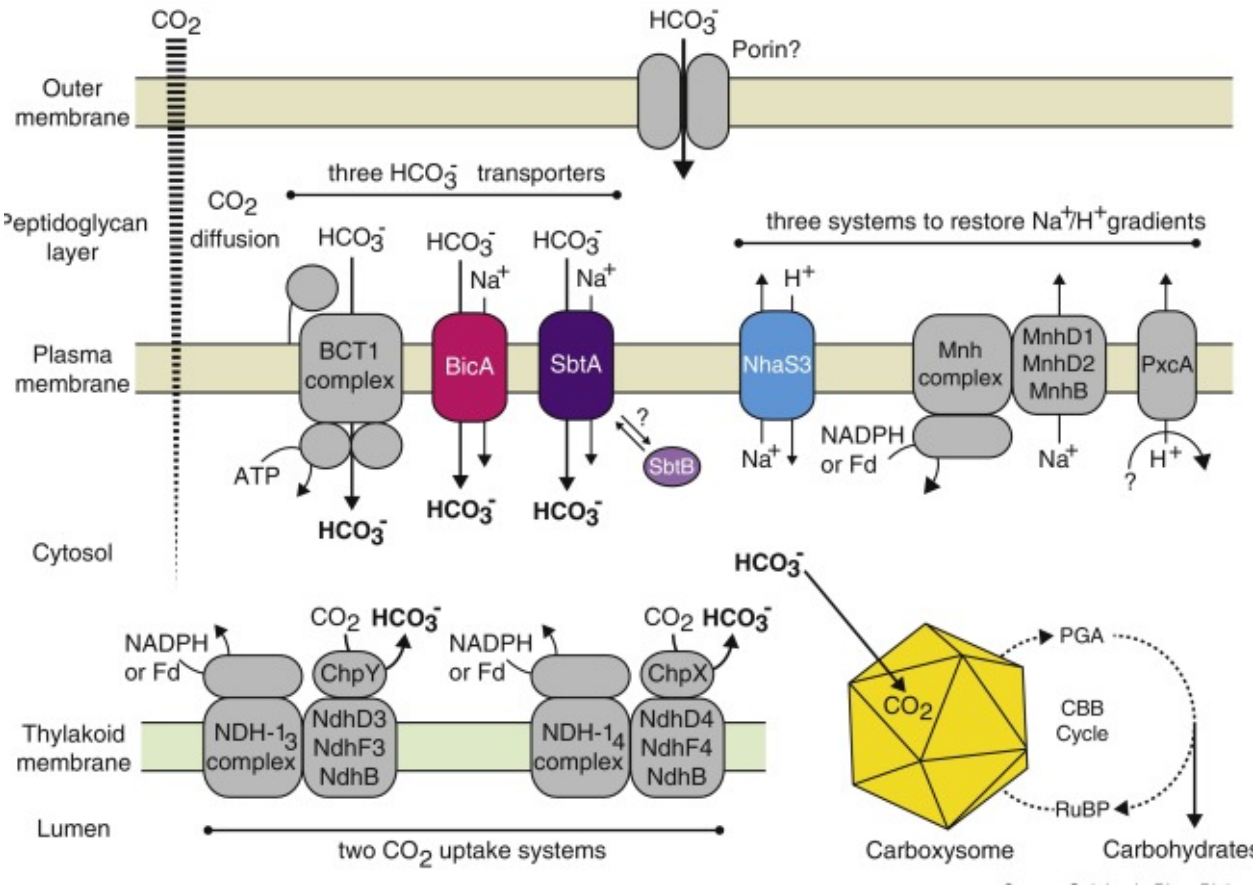

Figure 2. Schematic of *Synechococcus elongatus* sp PCC7942 Carbon Concentrating mechanism (CCM) describing the fates of inorganic carbon sources (CO_2 and HCO_3^-). The CCM includes passive diffusion of CO_2, three bicarbonate transports, and two CO_2 hydrating complexes. ChpY and ChpX are also known as CupA and CupB respectively. There are two sodium symport (BicA and SbtA) HCO_3^- transporters and one ABC-type transporter (BCT1). Bicarbonate is transported into the carboxysome (yellow) and, via a carbonic anhydrase, reconverted to CO_2. Rubisco is also housed in the carboxysome.

the case, and only occurs in my work when we aerate our cultures by bubbling with air supplemented with 5% CO_2. To augment passive diffusion, the second subsystem is employed by the cell which involves a membrane transport subsystem used to import bicarbonate across the cytoplasmic membrane. For this, most species of cyanobacteria have a triad of bicarbonate transporters known as BCT1, BicA, and SbtA. SbtA and BicA are sodium symports while BCT1 is an ATP-dependent bicarbonate transporter (Burnap et al., 2015; Price, Coleman, & Badger, 1992). These three transporters allow HCO_3^- to be pumped through the plasma membrane into the cytosol of the cell. Bicarbonate can then enter the carboxysome, which houses RuBisCO, and via carbonic anhydrase, the bicarbonate that diffuses into the carboxysome is converted to CO_2 in close proximity to the active site of RuBisCO. Inorganic carbon is present in two usable forms, bicarbonate and CO_2, under normal environmental conditions and with the relative abundances depending upon the pH (see figure about inorganic carbon). At pH8, a large portion of the total inorganic carbon is present as bicarbonate. This allows the cells to effectively rely on bicarbonate transporters as an efficient mechanism to carbonate the cell. However, if the cell resides in a lower environmental pH, the amount of available inorganic carbon present as bicarbonate decreases as it transitions to the third subsystem, which is the biochemical uptake CO_2. If a cell is in a C_i limited environment of a pH7 or lower, as is sometimes found in nature, it can use its CO_2 uptake systems (Cup), which are capable of using redox energy to drive the conversion of CO_2 to bicarbonate. Research also suggests that another main function of the CO_2 hydrating complexes is to recycle CO_2 that has leaked from the carboxysome. If CO_2 cannot be bound by RuBisCO in the carboxysome, then it is also prone to leakage, as it appears to rapidly diffuse back into the cytosol where it is prone to leakage from the cell (Ding et al., 2013).

The CO_2 uptake systems uses modified NADH dehydrogenase oxidoreductase (NDH-$1_{3,4}$) to hydrate CO_2 to the more biochemically utilizable bicarbonate (Ohkawa, Price, Badger, & Ogawa, 2000; Shibata et al., 2001b). NADH dehydrogenase oxidoreductase (i.e. Complex I) is normally found in the mitochondrial respiratory chain. Complex I serves a couple important functions in the respiratory chain. First, it oxidizes NADH and uses the derived electrons to reduce ubiquinol (Sharma, Lu, & Bai, 2009). Reduced ubiquinol goes through a cascade of events that ultimately result in the pumping of protons across a membrane which can later be used to power ATP synthase. The cyanobacterium uses a remarkably similar membrane protein complex to power its CO_2-hydrating mechanisms, although the details of this remain to be clarified and, indeed, my thesis aims to help in this direction. Cyanobacteria employ a homologus protein complex to Complex I, with the most substantial differences being in the electron donor/acceptor and, of course the CO_2-hydrating portion. Instead of performing redox chemistry with NADH and ubiquinol, ferredoxin is oxidized and plastoquinone is reduced. This, hypothetically, results in the shuttling of protons across the thylakoid membrane, establishing a proton gradient as with respiratory complex I.

1.5 Carbon Dioxide Hydration

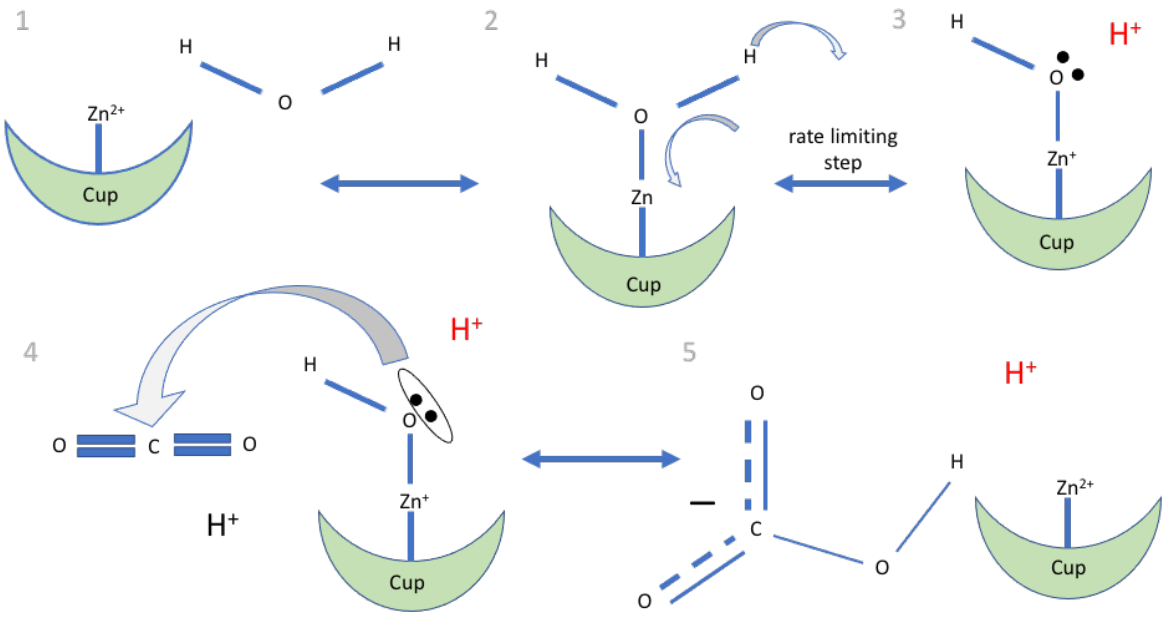

Figure 3. Biochemical Mechanism of CO_2 Hydrating Proteins (shown in green) exabit how the protein binds and hydrates CO_2. Proton (H^+) dissociation shown in red happens upon the creation of the hydroxide anion intermediate step (Step 3). Additional H^+ shown in step 4 & 5 is the same H^+ from step 3.

Interestingly, it appears that cyanobacteria have evolved a mechanism to harness this proton-pumping power in order to couple the classical redox chemistry used in NDH-1 to insure a nearly unidirectional carbonic anhydrase-like activity of Cup(Ohkawa, Pakrasi, & Ogawa, 2000). As depicted in figure 2, this cup protein is found on the cytoplasmic side of the thylakoid membrane across from the peripheral arm. It is understood that these proteins facilitate the reversible CO_2 hydration reaction described below (figure 3).

$$CO_2 + H_2O \rightleftarrows HCO_3^- + H^+$$

It is understood that the Cup protein is responsible for facilitating a reaction similar to that of a carbonic anhydrase. A common feature of all classes of CA is the presence of a metal cofactor active site. Through the help of the recently solved crystal structure, it is observed that the Cup protein is no exception (Schuller et al., 2020). In this particular case, the Cup proteins coordinate a zinc (Zn). This coordinated Zn ion is capable of binding a water molecule at the electronegative oxygen. At the formation of this bond, the electron density existing in the unbound water molecule promptly shifts during the formation of the Zn/O^- ligand bond. The shift in electron density in the water molecule, weakens the binding of the proton on the distal hydrogen, decreases its pK_a and thus allows for the dissociation of a proton. This creates a hydroxide anion intermediate along with a free proton. It is thought that the production of this hydroxide anion intermediate is the rate limiting step in a remarkably quick reaction. In the presence of a CO_2 molecule, the hydroxide anion intermediate performs a nucleophilic attack on the electrophilic carbon on the CO_2. This reaction promptly creates a molecule of bicarbonate, which is displaced by an incoming water molecule, thus freeing up the active site of the Cup protein, leaving a free proton as a "byproduct". This reaction accruing at the active site of the Cup protein, combined with redox chemistry occurring on opposite peripheral membrane protein subunit, also known as the L-module, allow for the cell to produce bicarbonate in an energized fashion, although the mechanism coupling electron transfer to proton pumping and CO_2-hydration remain to be clarified. The NDH-1_4, as well as the NDH-1_3, is a modified NADH dehydrogenase oxidoreductase, that functions akin to Complex I of the respiratory chain on the L module.

1.6 Complex I/NDH-1_4 Homology

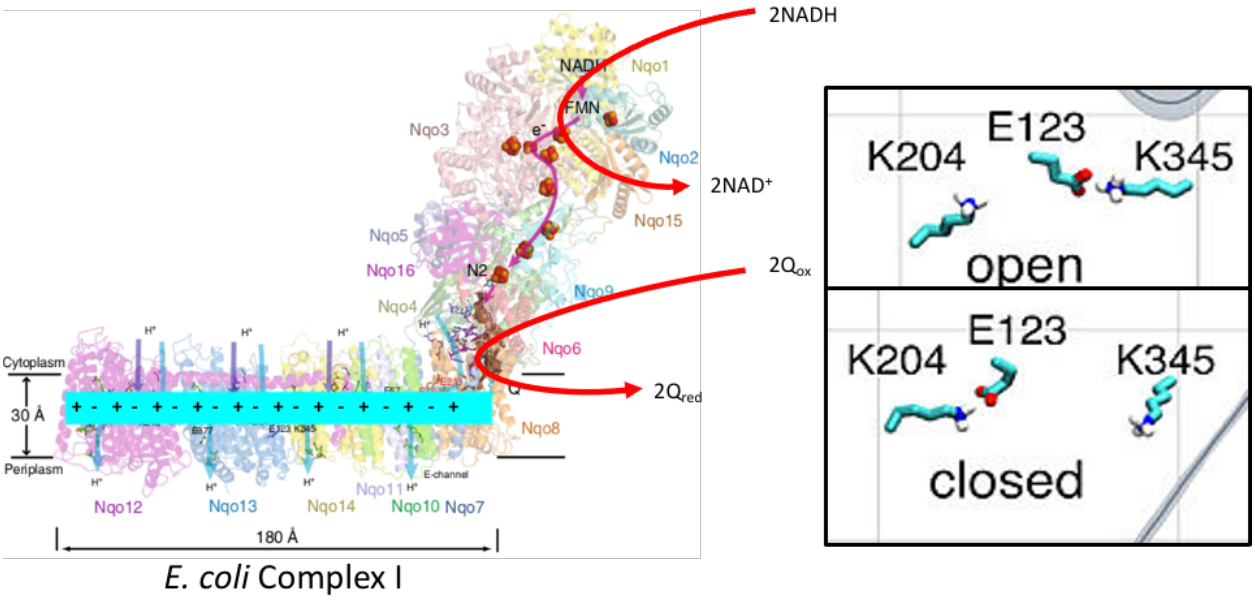

Figure 4. Structure/Function of Escherichia Coli Respiratory Complex I including proton pumping and coupled redox reactions, similar to that found in NDH-1_4. Exceptions include initial reductant and extended L-module (left). Hypothetical interactions of charged (I.E. acidic or basic) amino acid residues along charge relay system (right).

To understand the biochemical complexity of the NDH-$1_{3,4}$ complexes, it is first essential to understand the molecular mechanism of Complex I (Figure 4). In Complex I, NADH is oxidized with the sequential dontation of electrons to a series of iron sulfur clusters and eventually to Coenzyme Q located near the membrane proteins. Once Coenzyme Q is reduced, its chemical and physical conformation is altered in ways that remain to be experimentally clarified. Current hypotheses contend that this reduction event induces a change in charge, and therefore conformation, of key critical residues nearby the quinone reduction site and then to an extended set of charged residues running along the membrane-bound portion of the complex(Gutiérrez-Fernández et al., 2020). The initial reduction of the quinone is proposed to

induce a sequential set of changes of pK_a, akin to a domino effect, in a linear array of critical charged residues running along the center of membrane-bound antiporter-like, proton-pumping subunits (Figure 5)(Parey et al., 2021). These membrane-bound subunits in Complex I are responsible for the pumping of protons across the membrane according to mutagenesis and biophysical studies (Mühlbauer et al., 2020; Nakamaru-Ogiso et al., 2010; Sato, Torres-Bacete, Sinha, Matsuno-Yagi, & Yagi, 2014; Torres-Bacete, Nakamaru-Ogiso, Matsuno-Yagi, & Yagi,

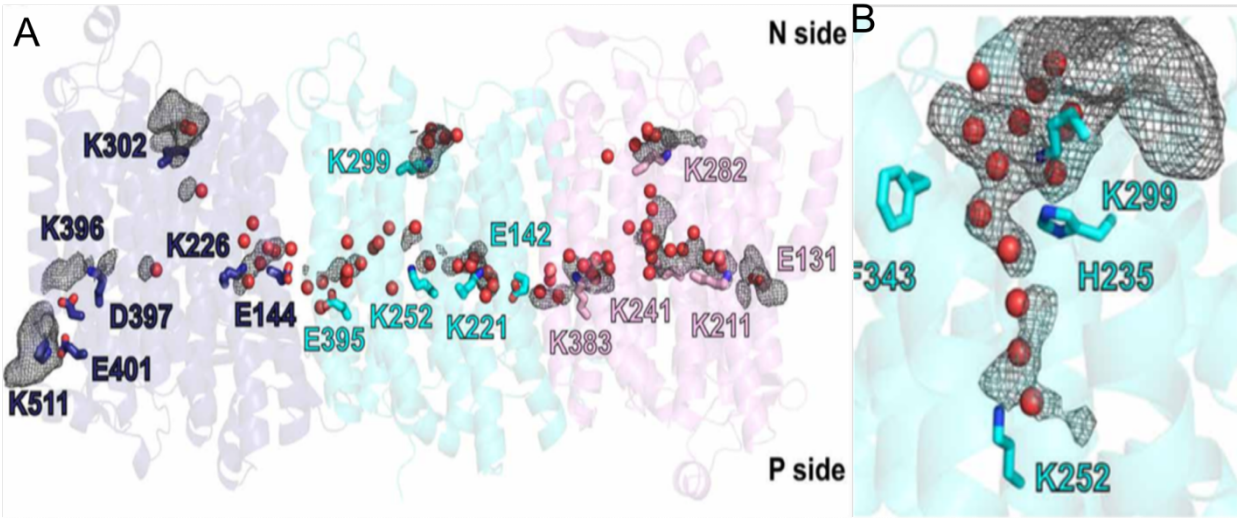

Figure 5. Patterns of hydration (Red) in *Yarrowia lipolytica* as well as identified critical proton pumping residues elucidate regions of potential interest as it relates to NDH-1[4]. A) Shows a detailed characterization of critical proton pumping residues located in the water wire of complex I B) Shows an area of potential proton trapping/translocating before proton/water wire interaction.

2007). This proton pumping in, not only Complex I, but other protein complexes in the respiratory chain including cytochrome b-c_1 and cytochrome oxidase, allow for the establishment of a proton gradient. This can power ATP synthase, producing ample amount of the high energy ATP molecule. The critical residues in each antiporter-like subunit are responsible for shuttling and trapping the proton inside the membrane in response to changes in nearby charged residues in the chain. When the redox reactions trigger the

conformation/pKa change in the charge relay system, an individual residue interacting with a neighboring residue of the opposite charge will no longer have the charge characteristic needed to maintain that interaction. This will promote a neighboring residue to dissociate from the ionic interaction, adopt a new conformation swinging over to interact with its directly opposite amino acid, forming a new electrostatic interaction. In the process, pKa changes are combined with gating mechanisms to promote the release of proton previously bound from the N-side of the membrane, to be released to the P-side of the membrane. According to this model, this process, repeated sequentially down the array of adjacent charge resides, will produce a

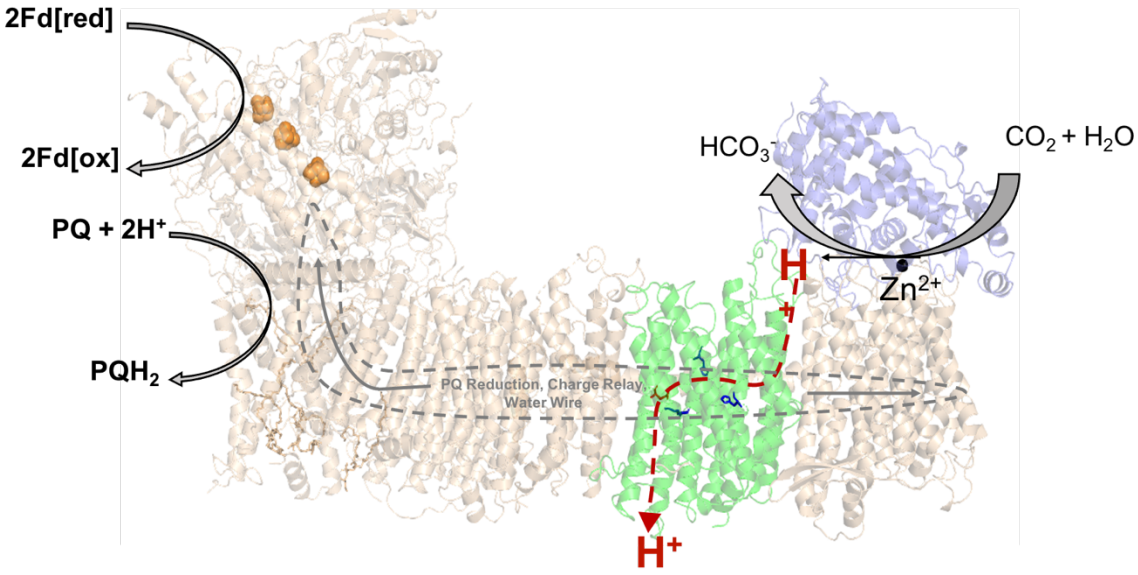

Figure 6. Hypothesized protein pumping and CO_2 hydrating system in the NDH-1_4 protein complex. CupB (purple) shows the mechanism of the CO_2 hydration reaction coupled with the redox chemistry starting at a triad of iron sulfur clusters (orange)**.** This allows for the proton pumping of membrane bound subunits including NdhD4 (green).

scissoring-like functional motion, similar to that depicted in figure 4, along the interior of the protein complex. This scissoring motion (due to the shift in pKa) allows the proton to dissociate and be ejected to the P-side of the membrane. The overall function of Complex I is to pump

protons, establish a proton gradient, and power respiration by fueling ATP synthase. NDH-1_4 is hypothesized to function similarly to complex I, harnessing the redox energy of the L-Module and coupling that reaction to remove the proton from the active side of CupA (Figure 6). Instead of using NADH and ubiquinone, NDH-1_4 uses reduced ferredoxin and plastoquinone. Similar redox chemistry takes place, allowing the same proton pumping actions to occur. It is thought that there are critical residues in NdhD4 that are essential for the complex to trap and remove the proton produced from the CO_2 hydration reaction fast enough for the hydroxide anion intermediate to react with a CO_2 molecule. This product removal mechanism would allow the reaction from CO_2 to HCO_3^- to proceed in an energized fashion, disallowing the reverse reaction back into CO_2 at the rate limiting hydroxide anion intermediate stage.

1.7 Questions/Goals

While the CO_2 uptake system found in cyanobacteria is interesting considering it is essential for its survival, especially in CO_2 starved environments, the molecular mechanics of this unique system also holds exciting biotechnological promise. Due to the ever-increasing concentration of the greenhouse gas CO_2 in Earth's atmosphere, the worldwide climate crisis is as urgent of a problem as it has ever been. There are many potential solutions, one of which could lie in understanding the functionality of the CO_2 hydrating complexes in cyanobacteria. While the

function of the Cup proteins in the CO_2 hydrating complexes is currently being solved, little is known about the function of the rest of the complex. Understanding how the NdhD4 subunit of this complex works, could provide a framework for elucidating how the complex works as a whole. It is our hypothesis that the NdhD4 subunit functions, at least in part, to pump protons across the thylakoid membrane, which would allow for product removal away from the active site of CupB, thus energizing the reaction in favor of HCO_3^- formation. We hypothesize that it does this through the previously stated, charge relay/shuttle gate mechanism. According to our hypothesis, there are critical residues, specifically charged residues, in the NdhD4 protein that are responsible for this proton translocation. Using structural modeling and amino acid sequence alignments, it is possible to infer these residues based on the extensives studies on the homologous subunits of the *E. coli* and other Complex I respiratory complexes.

The goals of this study were

- Develop a recipient deletion mutant strain, Δ*ndhD4*, missing the NdhD4 protein subunit.
- Construct and test an expression plasmid that allows for the complementation of the Δ*ndhD4* strain with a functional *ndhD4* gene
- Use site-directed mutagenesis on the complementing plasmid to introduce point mutations at potential critical residues for the hypothesized proton pumping mechanism.

CHAPTER II

EXPERIMENTAL PROCEDURES

2.1 Growth Conditions

Wild type *Synechococcus elongatus* sp. PCC7942 (S7942) (as well as mutants) were plated and propagated from frozen glycerol stocks onto sterile nutrient rich media at pH8, buffered with 10 mM HEPES-NaOH, referred to as BG-11. BG-11 is a cocktail of minerals and inorganic cofactors, such as ammonium iron citrate, that allows for optimal growth of cyanobacteria. BG-11 media can be combined with 1.5% Bactoagar to propagate cells on plates or can be used as a liquid media to harvest relatively large amounts of cells for genomic or physiological experiments. All cells were grown at 31º Celsius (ºC) under approximately 60 µmol m^{-2} s^{-1} photons provided by a cool white F30 florescent lamps. When in liquid shaking culture, the cultures of 100 mL in 250 mL Erlenmeyer flasks were kept constantly shaking at 180 rpm under continuous illumination. Cells needed for physiological assays or cells containing severe damage to the CCM (ΔA/B) were supplemented with 5% CO_2 in order to insure proper growth. 5% CO_2 was defined as the high C_i conditions given that at pH8 HCO_3^- and CO_2 are presumed to be present in abundance. Antibiotics (Table 1), at all times, were applied under a consistent concentration, with the exception of cell that were used in physiological experiments.

2.1.2 Experimental Growth Conditions/Applications

For cells to be used in experimental analysis, particularly experimental analysis on the NDH-1_4 complex, cells were treated in a very particular fission. Starter cultures were grown as listed above, propagate from plates. When $O.D._{750}$ of starter cultures reached about 0.7, the cells were harvested and inoculated in 800 mL BG-11 cultures at pH8 to an $O.D._{750}$ of 0.04. Cells were supplemented with 5% CO_2 and grown under high light conditions. These cells were grown for 45-48 hours and harvested at an $O.D._{750}$<1.0. After harvest, the cells were resuspended to a Chl concentration of 50µg/mL and allowed to rest for about an hour, shaking gently under soft white light. Before experimentation, the cells were washed and resuspended with C_i-free Bis-Tris Propane (BTP) Buffer. To make BTP buffer hydrochloric acid 2.0N is mixed in deionized water to a concentration of 1.339 g/mol and allowed to bubble gently with nitrogen gas for 20 minutes. After this BIS-TRIS propane is added and mixed to a concentration of 50 mM. After the BTP powder is completely desolved, the solution was added to a flask and capped with a rubber stopper to prevent gas exchange. The goal of this buffer is to drive off all remaining C_i from the BG-11 media in which the cells were resuspended in. Then cells were supplemented, in a different manners, with $KHCO_3$ and carbonic anhydrase. The goal of these additions is to force the cell to use its CO_2 hydrating mechanisms with out relying on the sodium dependent bicarbonate transporters (hens the addition of $KHCO_3$ not $NaHCO_3$).

2.2 Strains and Molecular Construct Detailed Explanation

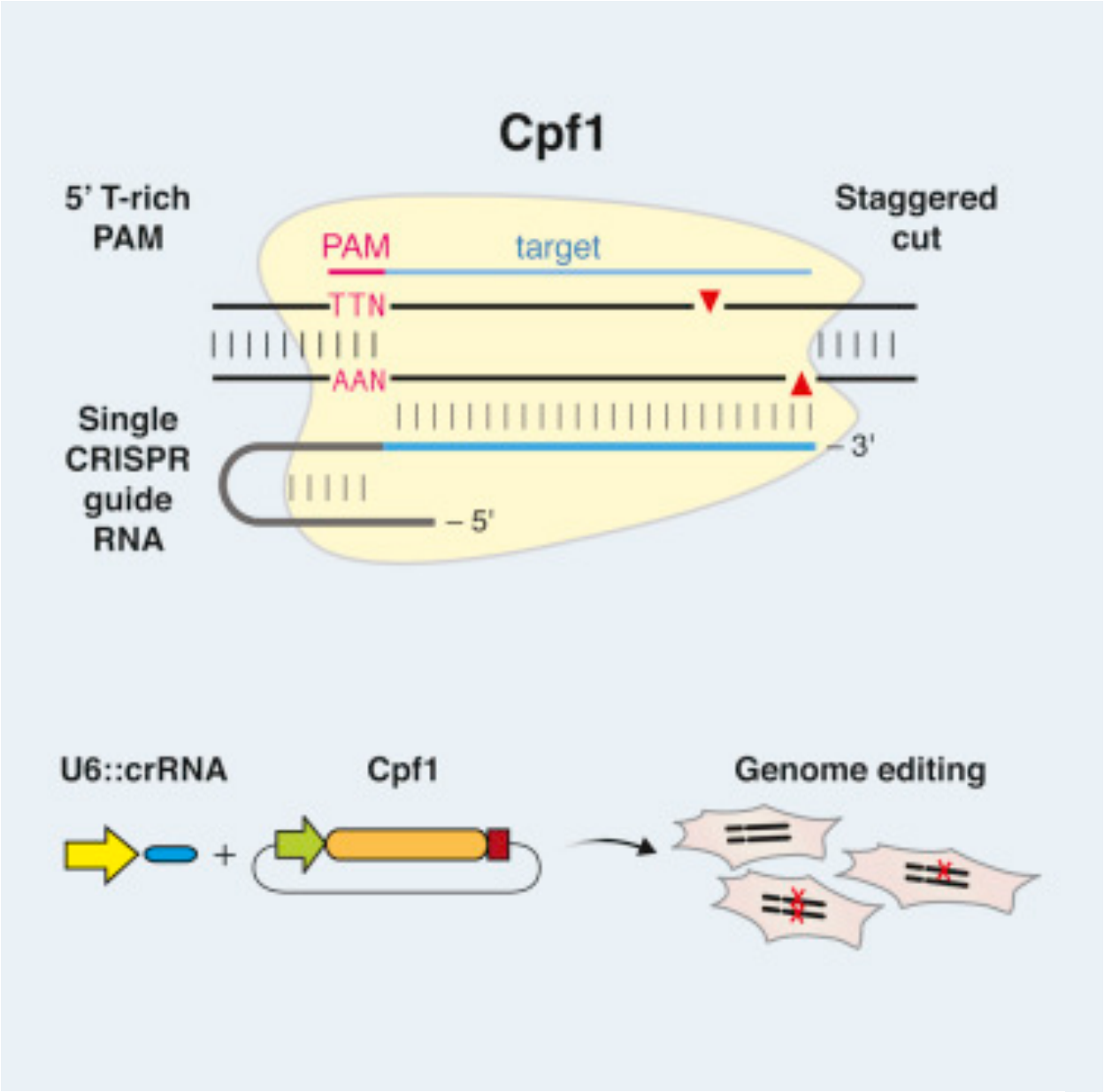

Figure 7. Molecular mechanism of Cpf1 enzyme for DNA cutting with visualization of functionality of PAM stie in Cpf1 protein and the guide RNA, which is not part of the Cpf1 protein.

2.2.1 Construction of *ΔndhD4*

The initial step in probing the characteristics of a protein of interest in a structure/function study is to create a deletion of the gene of interest. The first mutant created for this study was

a *ndhD4* knockout in S7942 genetic background. This was accomplished through the employment of the CRISPR-Cpf1 genome editing plasmid. This plasmid, similar to CRISPR-Cas9, has the ability to make site-directed double stranded breaks in the genome that can then be reannealed and repaired to create a markerless gene deletion (Jiang et al., 2017).

As previously stated, the Cpf1 enzyme is capable of making double-stranded breaks and reannealing the DNA to create a markerless gene deletion. To do this, the CRISPR plasmid is introduced into the cell where it then undergoes transcription and translation to produce the Cpf1 enzyme which is encoded for in the plasmid (Figure 7). Also encoded in this plasmid is a guide RNA (crRNA) that shares homology with the coding strand of the genomic DNA, thus guiding the enzyme by binding to the template strand. This short genetic sequence can be changed via restriction sites, BsaI, on the plasmid (Figure 7). Once the crRNA guides the enzyme to the DNA, the protospacer adjacent motif (PAM) allows the enzyme to make double stranded cuts at specific sites (Figure 9). Once the cuts are made, the CRISPR plasmid contains homologous repair templates that are inserted via restriction digestion and Gibson assembly through the BamHI restriction enzyme (Figure 7). Homologues recombination templates can be cloned into the plasmid, allowing the cell to 'heal' the double stranded breaks created by the Cpf1 enzyme.

The unique plasmid responsible for genome editing was created by modifying a CRISPR-Cpf1 backbone plasmid (Niu et al., 2019; Ungerer & Pakrasi, 2016). The crRNA was inserted in between the BsaI restriction sites. Around 500 ng of plasmid DNA was mixed with an appropriate amount of BsaI (designated by manufacturer, New England Biolabs). The mixture,

buffered with Cutsmart ® Buffer, was incubated at 37 ºC for two hours. The product was then analyzed on a gel to verify enzyme digestion was successful. The linearized plasmid was then cloned via Gibson Assembly with the desired genetic sequence produced via polymerase chain reaction. The same process was used to insert the sequences for homologous recombination into the plasmid. For this digestion and sequential Gibson Assembly, the enzyme BamHI was used to linearize the plasmid. This reaction was buffered in Cutsmart® and incubated at 37 ºC for two hours.

To introduce the plasmid into S7942, a tri-parental bacterial conjugation between two *E. coli* strains and the recipient S7942 was performed. The conjugation was facilitated by helper plasmids pRL443 and pRL623, along with the CRISPR Cpf1 plasmid . Each plasmid (pRL443, pRL623, and CRISPR Cpf1) was housed in a separate *E. coli* strains. All plasmids were genetically engineered and housed in *E. coli*. Two cultures were inoculated in LB. Once culture contained the strain containing the pRL443 plasmid. The other was inoculated with a combination of the CRISPR-Cpf1 plasmid and the pRL623 helper plasmid. pRL443, pRL623, and CRISPR_Cpf1 possessed antibiotic resistance cassettes to ampicillin, chloramphenicol, and spectinomycin respectively. The cultures were applied with their respective antibiotics and incubated overnight at 37 ºC, shaking vigorously. The following morning, the cultures were pelleted and washed three times with 10 ml of antibiotic-free LB. Each set of cells were then resuspended in 60 ul of LB and mixed together. Meanwhile, a culture of S7942 was grown to late linear phase (around $O.D._{750}$ of 0.70). The cyanobacteria was pelleted via centrifugation at 6,000 times gravity (xg) for seven minutes. The pellet was gently resuspended to preserve pili in 500 ul of BG-11 and analyzed for Chl concentration. The entirety of the *E. coli* mixture was then

combined with an appropriate volume of cyanobacteria equivalent to 10 μg of Chl. The slurry was then plated on a combination of BG-11 and LB agar plates for one day, followed by BG-11 agar media lacking antibiotic selection, finishing with BG-11 agar media containing the desired selective pressure (spectinomycin).

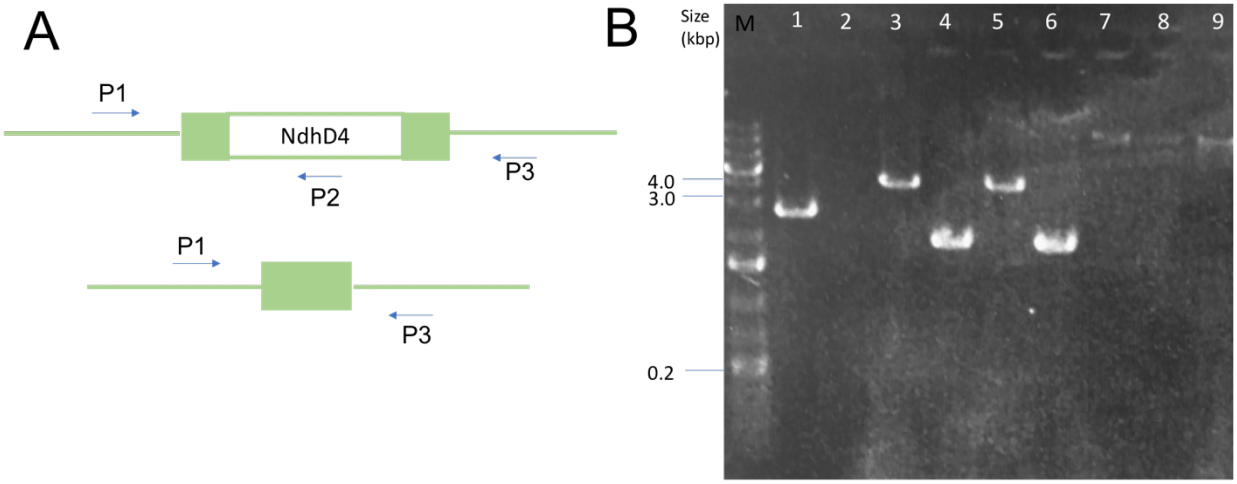

Figure 8. Construct Conformation of ΔNdhD4 with Gel Electrophoresis. A) Primer design for verification of gene deletion. P1 and P3 are primers that flank the NdhD4 gene and P1 and P2 are primer pairs that will amplify only if the NdhD4 gene is present, as P2 binds specifically to the gene B) Segments of DNA amplified by polymerase chain reaction include primer set 1 in lanes 1,3,5 and primer set 2 in lanes 2,4,6. Lanes 1 and 2 include DNA from a colony conjugated with CRISPR plasmid with a successful gene deletion. Lanes 3,4 feature DNA of a colony conjugated with CRISPR plasmid with an unsuccessful gene deletion. Lanes 5 and 6 feature DNA from WT S7942.

After the entirety of the conjugation procedure, the cells were allowed to grow until visible colonies appeared. These colonies were harvested, cultured, and analyzed for successful gene deletions. To do this, primers were designed that facilitated a multiple pronged approach to insuring a successful gene deletion. One primer set (P1 and P3) was designed to completely flank the gene of interest and homologous recombination sites (Figure 8). The other primer set was designed to probe the presence, or absence, of the *ndhD4* gene itself (P1 and P2). The PCR reactions for each primer set were executed on the genomic DNA of multiple colonies produced

via the conjugation event and S7942 genomic DNA. The product was then stained and passed through and agarose gel via electrophoresis. The gel was then stained with Gel Green and imaged (Figure 8). If the genome maintained the *ndhD4* gene, the expectation would be that primer set P1/P3 would exhibit a band at 4.2 kilobase pairs (kbp) and the primer set P1/P2 would exhibit a band at 1.9 kbp. However, if the *ndhD4* gene was successfully removed from the genome the

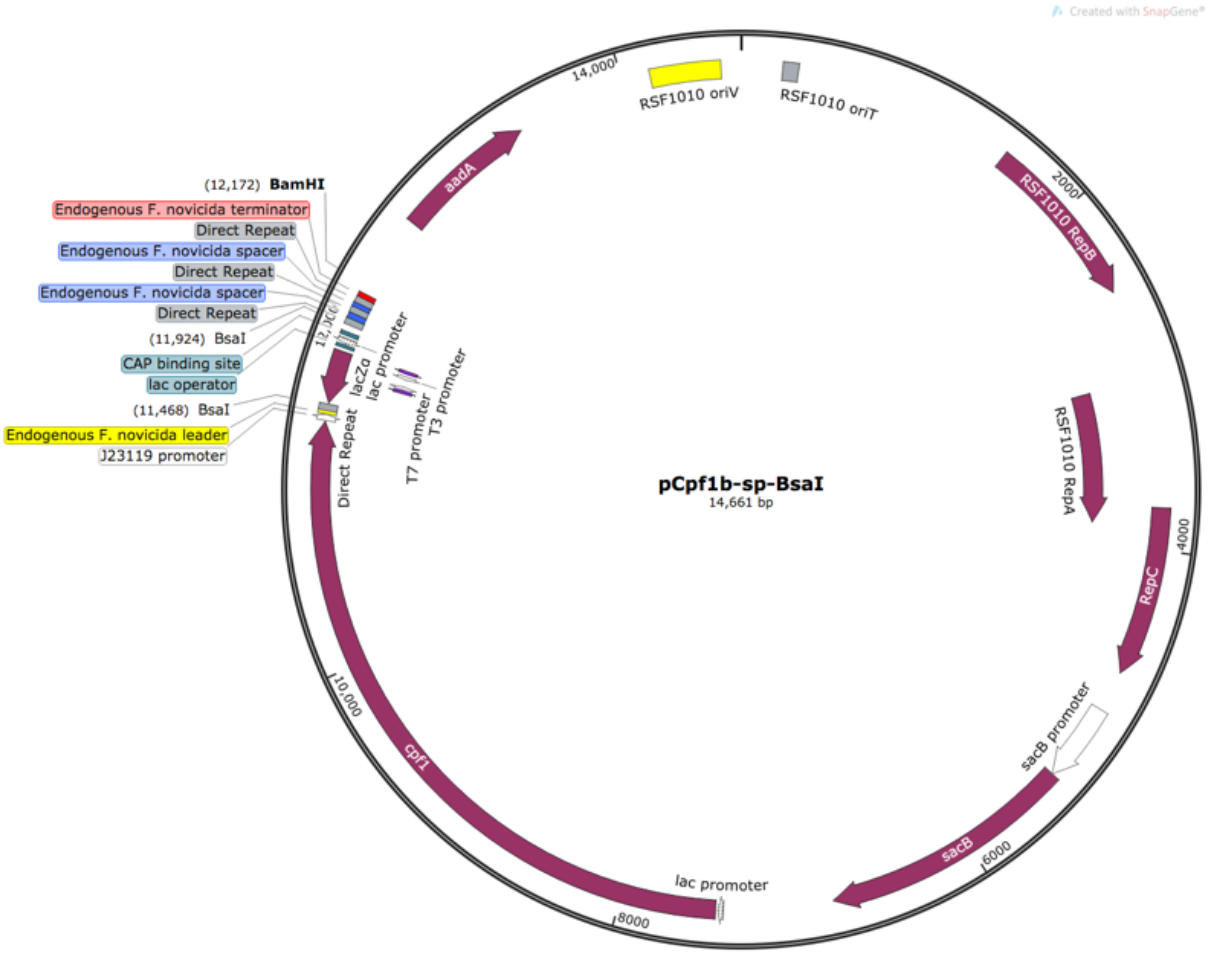

Figure 9. Snapgene Map of All-in-One CRISPR-Cpf1 gene deletion system A) Empty plasmid before addition of upstream and downstream homologous recombination regions. Map includes gene for Cpf1 enzyme and site-specific guide RNA.

expectation would be that primer set P1/P3 would feature a band at 2.7 kbp and primer set P1/P2 should not result in any amplification. In Figure 8b, colony 4 probed in lane one and two shows the bands that would be expected if the *ndhD4* gene was deleted.

2.2.2 Δ*ndhD4* –CRISPR Plasmid Cure

The CRISPR – Cpf1 gene modification system allowed for markerless gene deletions. While this is a beneficial tool to use, as it does not require the use of an antibiotic cassette as a standard gene knockout via homologous recombination would, however, the all-in-one CRISPR plasmid must be removed, along with the antibiotic cassette it houses, after the completion of a succesfull gene modification. If not removed, the strain will maintain the plasmid and the antibiotic resistance, which potentially interferes with downstream procedures such as transformation with the complementation plasmid. The plasmid is designed with a *sac*B gene. When expressed, the gene produces an enzyme known as lavansucrase. Levansucrase will produce a toxic metabolite in gram-negative bacteria in the presence of sucrose. This allowed for selection of individual cells that have lost the CRISPR plasmid, as they will no longer be expressing the *sacB* gene and therefore no longer producing levansucrase. Unfortunately, there is evidence that *Synechococcus elongatus* PCC 7942 is sensitive to media containing 5% sucrose, probably because this strain uses sucrose as a compatible osmolyte. To avoid this issue while still successfully curing the plasmid, a different method of curing involving replica plating was used. To cure this strain of the gene-editing plasmid, a culture was grown to an $OD_{750} > 1.0$. A sample of this culture was then diluted 1:10,000 in standard liquid BG-11. 100 µL of this dilution was then plated on non-selective BG-11 agar plates. This plate was then allowed to incubate in

standard air conditions until colonies appeared. Once colonies were visibly present, between 100-150 were selected and spot-streaked in an ordered array on non-selective BG-11 media. These spot-streaks were allowed to grow for 7-10 days. After incubation, a sample of each spot-steak was re-streaked on selective BG-11 media then allowed to rest at room temperature. In this case, the selective marker on the CRISPR-cpf1 plasmid was spectinomycin. These plates were allowed to incubate for 7-10 days. Streaks that did not grow were presumed to not poses the antibiotic resistance gene and therefore not possess the CRISPR-Cpf1 gene editing plasmid.

2.2.3 Δ*ndhD4* Complement Strains - Δ*ndhD4*/pSE4Km_NdhD4 & ΔNdhD4/pSE4Km_NdhD4

Upon construction of the *ndhD4* knockout mutant (Δ*ndhD4*) two variants of complement plasmids were introduced, pSE4Km_NdhD4 and pSE4Km_NdhD4_NTST. Both plasmids served the same function, to complement the *ndhD4* gene back into the *ndhD4* mutant. Each plasmid was introduced via genetic transformation into two different cultures of Δ*ndhD4* , yielding two slightly different strains. The compliment strain containing the twin strep tag (NTST) was constructed to provide a mechanism of protein quantifications. This strain exibitied protein expression of NdhD4 with lack of dectable NTST accumulation, reslting in an uncessfull proteomic evaluation system.

Both plasmids were constructed from a variation of the same shuttle vector housing a CupB genetic cassette. The original pSE4 plasmid was constructed by Prof. Dean Price and is capable of replication in both *E. coli* and S7942 and is thus a shuttle vector (Price, Woodger, Badger, Howitt, & Tucker, 2004). The strains were modified using restriction digestion and sequential Gibson Assembly of the *ndhD4* gene, amplified from S7942 genomic DNA via the polymerase

chain reaction (PCR). The plasmid was designed to have three unique restriction sites. Two of these restriction sites, NcoI and SacI, were positioned at the N-terminus of the *ndhD4* gene. The unique location of these two restrictions sites, in combination with a C-terminus SacII, allow for the construction of the two similar but different shuttle vectors. One, pSE4Km_ndhD4, allows for the exclusion of a twin strep-tag, while the other, pSE4Km_ndhD4_NTST, allows for the twin strep-tag to be included in the expression plasmid.

Direct genetic transformation was the preferred method to introduce the shuttle vectors, pSE4 into Δ*ndhD4*. To ensure optimal transformation efficiency, the cells were grown to an $O.D_{750}$ of around 0.70 in 100 mL shaking BG-11 cultures. These cultures were grown under high carbon conditions (HC). Cultures were then harvested and resuspended by gently shaking in 1 mL of BG-11 liquid media. Once resuspended, more BG-11 media was added so that the current culture was brought to and $O.D_{750}$ of 2.5. For each transformation, 0.50 mL of cells at $O.D_{750}$ of 2.50 were placed in sterile test tubes or 15 mL falcon tubes. 10 µL of each plasmid DNA concentrated to at least 1 µg/µl was applied to the samples. The cultures were then allowed to sit at 31ºC under 60 µmol m^{-2} s^{-1} photons provided by a cool white F30 flourescent lamp for three hours. After three hours the tubes were shaken by hand briefly and allowed to sit for another two hours. The cultures were then plated separately on 0.45 µm nitrocellulose membrane filters. These nitrocellulose filters allow for the application of antibiotic in a stepwise fashion to the transformants. Starting out with no selective pressure, the transformants were then placed under one half the concentration of normal antibiotic selective pressure after one day, followed by full selective pressure three days after that. The antibiotic used for selective

pressure was kanamycin at a concentration of 20 µg/ml. Colonies were then harvested and propagated.

To ensure that both of the new complement strains were actively expressing the complement plasmids, plasmids were extracted from a cultures and re-introduced into *E. coli*. Both plasmids have origins of replications that are compatible in both *E. coli* and cyanobacteria, which allows for expression of the shuttle vector in both *E. coli* and S7942 (Ohashi et al., 2011; Price et al., 2004). Given that the plasmids contain two critical genes, the antibiotic resistance cassette providing selection and the gene of interest, this is a useful way to test the expression and function of NdhD4. To accomplish this, plasmid DNA was extracted from a culture of S7942 using a Midi plasmid prep kit (Omega Inc). The DNA was then precipitated and concentrated in

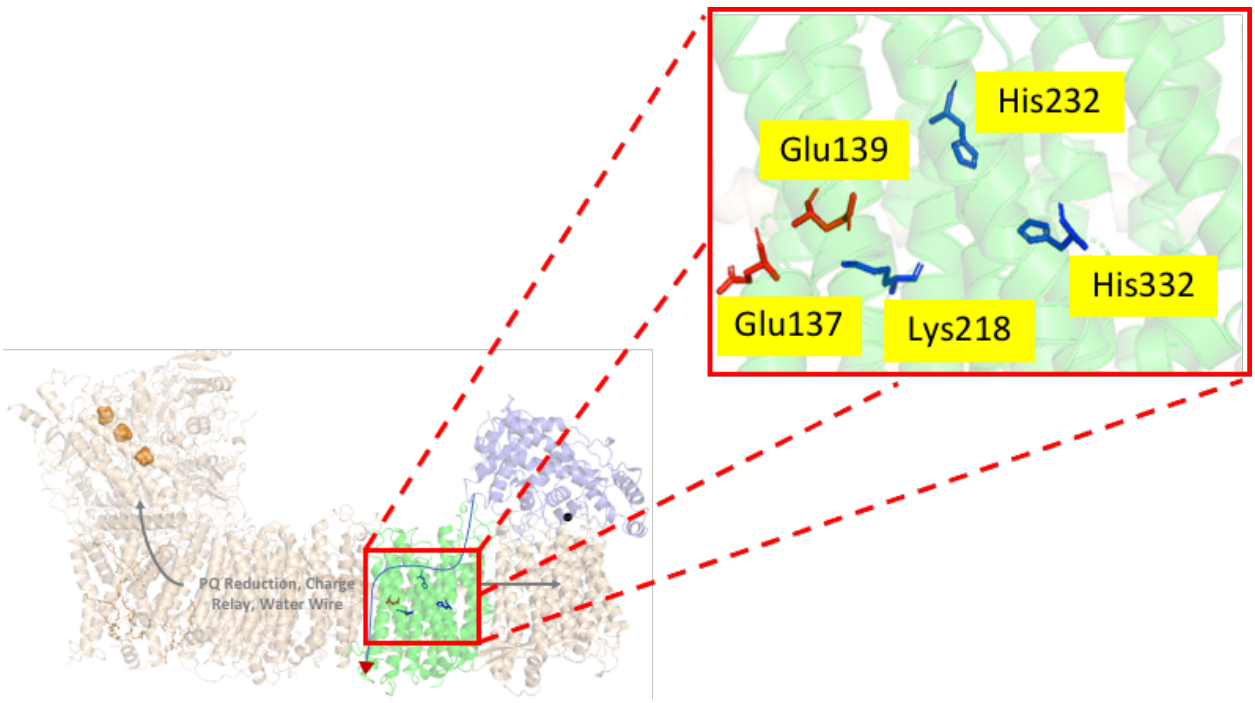

Figure 10. Residues selected for mutagenesis in the NdhD4 protein subunit of the NDH-1$_4$ CO_2 hydrating complex. Residues are hypothesized to be apart of the charge relay system (Glu137, Lys218, and Glu139) or along a potential proton path (His332, His232)

a minimal amount of Tris buffer. HB101 chemically competent *E. coli* cells were then transformed with the precipitated plasmid DNA. To accomplish this, the plasmid DNA resuspension of unknown concentration was mixed with the competent *E. coli*, heat shocked and allowed to incubate at 42°C for an hour in SOC media (Sambrook, 1989). The cells were then plated and allowed to incubate overnight. The presence of colonies under the appropriate antibiotic and lack of colonies on other antibiotics provides enough evidence to conclude that the cyanobacteria cultures do in fact contain the desired expression plasmids.

A series of desired point mutation were then selected (Figure 10) and the plasmid pSE4Km_NdhD4, which was used to create the WT control strain were harvested from *E. coli*, precipitated, and sent off to for modification at Genscript. This plasmid came back from Genscript containing the individual point mutations. Each point mutation was present only by itself and not with any other point mutation. Each of these point mutations were then transformed into DH5- alpha competent *E. coli* and frozen for storage. Similarly, each plasmid was sequentially transformed into the $\Delta ndhD4$ strain to allow for the expression of the variant *ndhD4* genes containing the desired mutations.

Once successful transformation of each strain was completed, the cells were initially grown to be flash frozen using liquid nitrogen and stored at -80°C for long term storage (Chen et al., 2016). Cells were then propagated on an initial plate. To do this, cells were quadrant streaked on BG-11 media containing bacto-agar and allowed to grow at 21°C under high light. Once done growing, plated cells were stored at room temperature under medium to low light. Only cells

from these plates were to be used for starter cultures. Plate cultures were restruck on fresh BG-11 plates when obvious and notable health of plated storage cells started to decline. A maximum of 4 restreaks were allowed to take place. After the fourth restreak, cells were grown up from frozen stock. This is in attempt to limit random mutagenesis/domestication of cells.

Table 1: Strain table of pertinent information regarding controls and mutants used in this work. The parent stran from which all mutand strains are made from is *Synechococcus elongatus* sp. PCC7942

Strain	**Common Name**	**Antibiotic Resistance**	**Genotype**
Δ*ndhD4*	ΔndhD4	None	Markerless Deletion of ndhD4
Δ*ndhD4*/pSE4-NdhD4	WT Control	Kanamycin (Km)	WT-Control (Complemented ndhD4)
Δ*ndhD4*/pSE4Km-NdhD4H332A	H332A	Kanamycin (Km)	Histidine→Alanine
Δ*ndh*D4/pSE4Km-ndhD4H232Y	H232Y	Kanamycin (Km)	Histidine→Tyrosine
Δ*ndh*D4/pSE4Km-ndhD4E139Q	E139Q	Kanamycin (Km)	Glutamic Acid→Glutamine
Δ*ndh*D4/pSE4Km-ndhD4K218E	K218E	Kanamycin (Km)	Lysine→Glutamic Acid
Δ*ndh*D4/pSE4Km-ndhD4E137Q	E137Q	Kanamycin (Km)	Glutamic Acid→Glutamine

2.4 Proteomic Evaluation

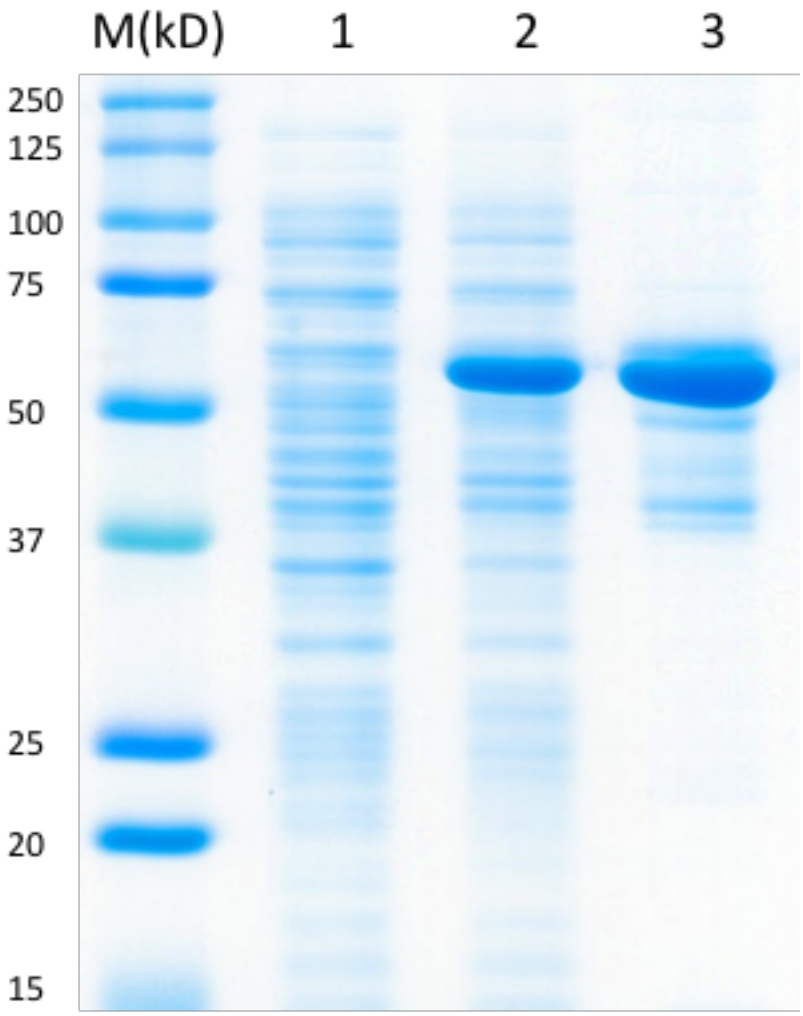

Figure 11. pMAL-NdhD4-HDs expression on SDS-PAGE Gel with Colloidal Blue Staining. Marker protein (M) is measured in kilodaltons (kD). Lane 1 is the whole proteome of e. coli containing the pMAL expression plasmid but not induced with IPTG. Lane 2 describes the same cells as in lane 1 but induced with IPTG. Hence the heavy band. Lane 3 describes the protein form lane 2 after is was ran through a column containing amylose.

Theoretically, amino acid substitution at critical residues in the protein subunit would have a functional effect on the photosynthetic physiology of the cell. This is opposed to a point mutation effecting the overall protein folding and accumulating ability of the subunit. To insure that site directed ammino acid substitutions are effecting the physiology from a biochemical

perspective rather than a structural standpoint, proteomic evaluation of membrane fractions were completed. To summarize, this includes the purification and visualization of membrane proteins in each individual strain, especially with regards to the NdhD4 membrane protein.

To accomplish this, we devised fusion protein containing the hydrophilic domains of the NdhD4 protein on both the N and P side of the membrane (figure11) with a maltose binding protein. This fusion protein was overexpressed in *E. coli* expression strain NEBexpress using IPT induction techniques. To accomplish this NEBexpression cells were transformed with the plasmid containing the fusion protein (figure12). Cells containing the plasmid were then grown to an $O.D._{600}$ of around 0.6. in two, 500 mL cultures. Then, IPTG was added and cells were allowed to incubate overnight at 18°C. Cells were then harvested and lysed via sonification. Once cells were broken, and clarified by centrifugation, the homogenate was added to amylose resin column and eluted with buffer containing maltose. This allows for the MBP to associate with the maltose, thus dissociating the fusion protein of interest, MBP-NdhD4-HDs.

Purified protein was harvested by cutting gel slices of large well blue native gels. (Figure 11 and 12) This product was then sent off to Pacific Immunology. Here, the company used the protein to create antibody against it in a rabbit host. The rabbit blood was then harvested, and the antibody was purified and shipped back.

Cells of both controls and all mutants were grown in both 5% CO_2 and Air. This differential C_i conditions allows for the investigation of not only the presence or absence of protein, but the differential protein expression considering the environmental conditions. NDH-1_4 has been shown to be a constitutively expressed complex, meaning that if membrane proteins in the

complex are present, they should be expressing at the same level across mutant strains and in variable C_i conditions.

Cultures were harvested and membrane fractions were purified. These fractions were ran on SDS gels and transferred to nitrocellulose paper via western blotting. From there, it was possible to probe the conditions of the NdhD4 accumulation using the NDhD4-HDs antibody and sequential secondary antibody via immunoblot analysis .

Subsequent work will involve purification of the MBP from the NdhD4-HD protein and production of antibody by my collegues in the lab using the procedure mentioned above.

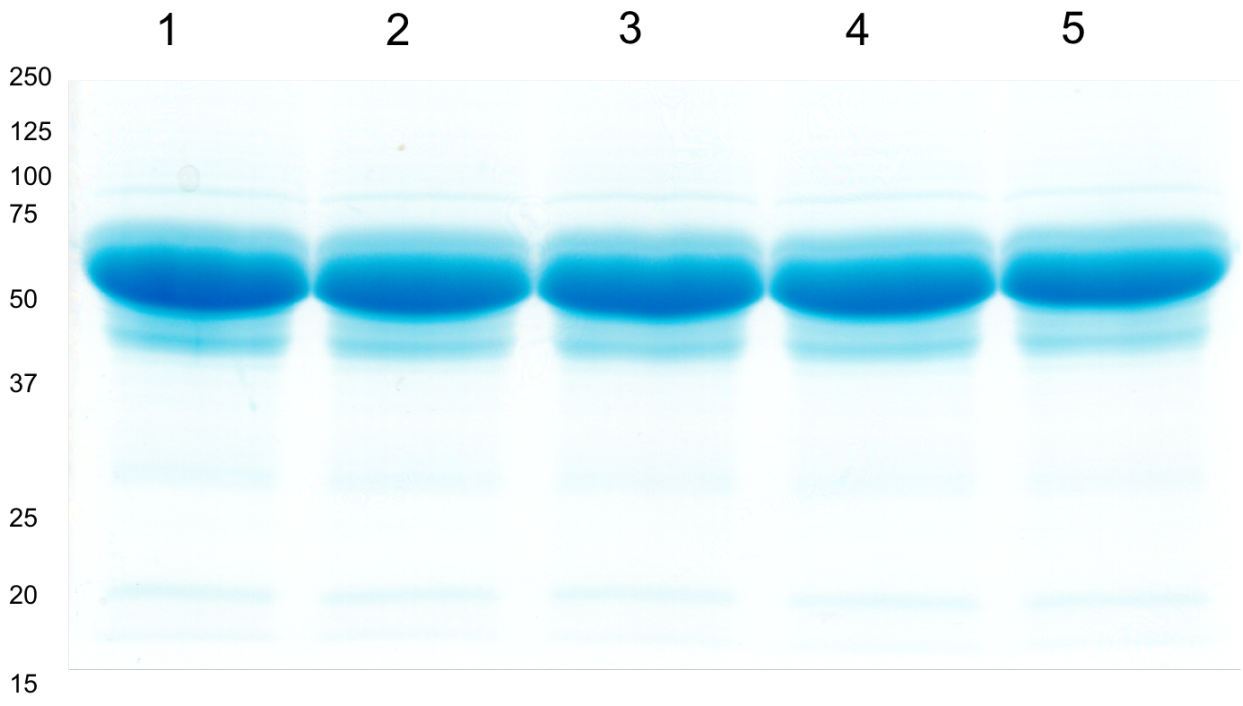

Figure 12. Purified Maltose Binding/ NdhD4HDs fusion protein after amylose column. All lanes are identical with 136 µg of protein in each well. pMAL-NdhD4-HDs is 61 kD (blue band) and NdhD4-HD's is theoretically 20kD**.**

CHAPTER III

PHENOTIPIC ASSAYS FOR NDHD4 DELETION AND COMPLEMENTATION STRAINS

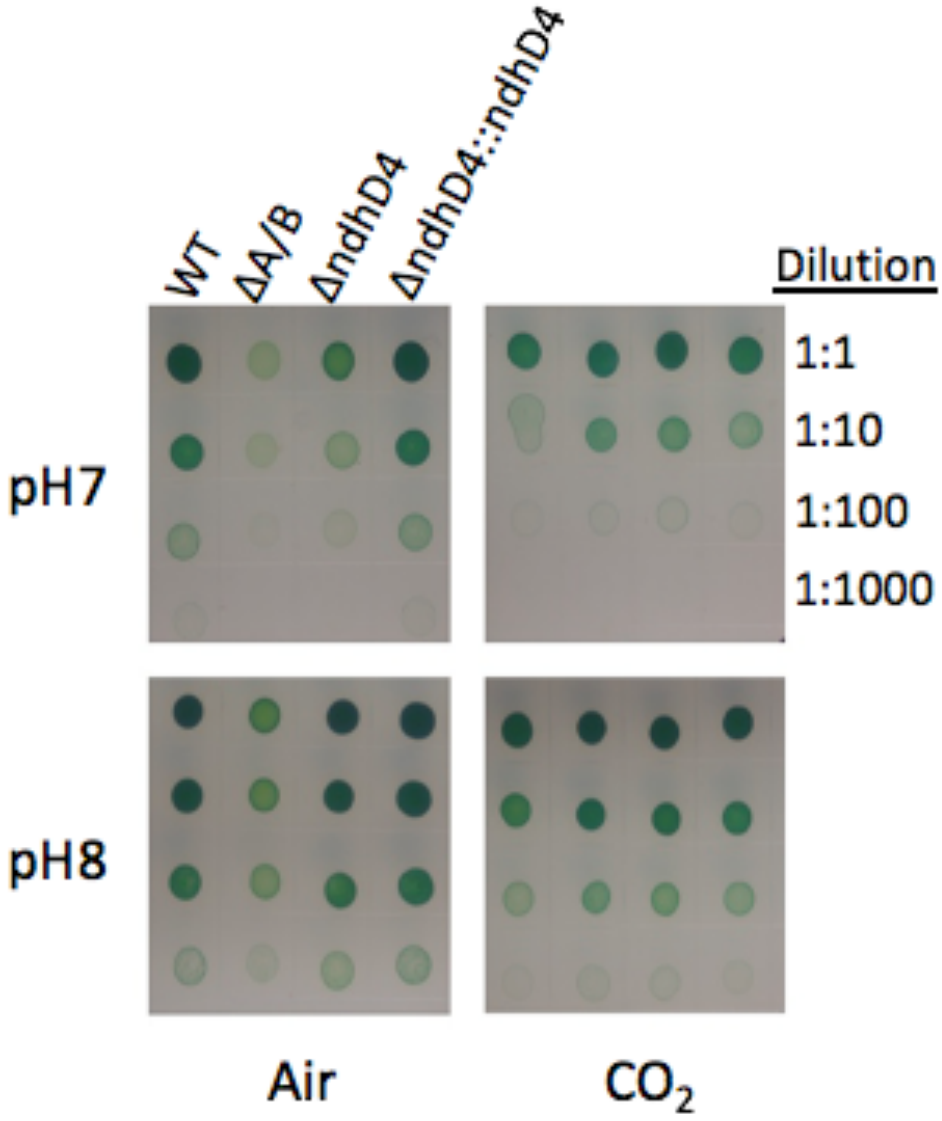

Figure 13. Spot Assay for autotrophic growth under differential C_i availability conditions BG-11 agar plates. Cells were grown to an $O.D._{750}$ of 0.7 in high CO_2 and pelleted via cointegration and resuspended to an $O.D._{750}$ of 1.0. Cells were then diluted with BG-11 to 0.1, 0.01, and 0.001. 7 µL of cells were used for each spot. Cells were allowed to grow for 5 days.

3.1 Spot Growth Assays to evaluate ndhD4 deletion and complementation strains

To initially assess if the gene is critical to the C_i concentrating ability of the cell, a spot-growth assay was performed. This assay allows for the analysis of general autotrophic growth under differential C_i conditions. Cells are grown under a combination of low (Air) or high (5% CO_2) environmental CO_2 and on growth media at either pH8 or pH7. Most importantly, cells grown in low environmental CO_2 on pH7 media best probe for the cells ability to rely on its CO_2 hydrating proteins. As seen in figure 13, WT and WT control strains show not only identical growth, but the best relative growth when compared to strains grown alongside them. In contrast, the strain labeled ΔA/ΔB, which describes a strain containing no CO_2 hydrating portions, has the relative lowest autotrophic growth. Autotrophic growth of Δ*ndhD4* is distinctly intermediate to that of the the WT and WT Control and the ΔA/ΔB strain. This result indicated the need for further exploration, given that there is differential growth capability's across these strains. This indicates that the changes made to the cells CO_2 hydrating ability have a unique and distinctive effect on the photosynthetic process.

3.2 CO_2 uptake assays to evaluate ndhD4 deletion and complementation strains

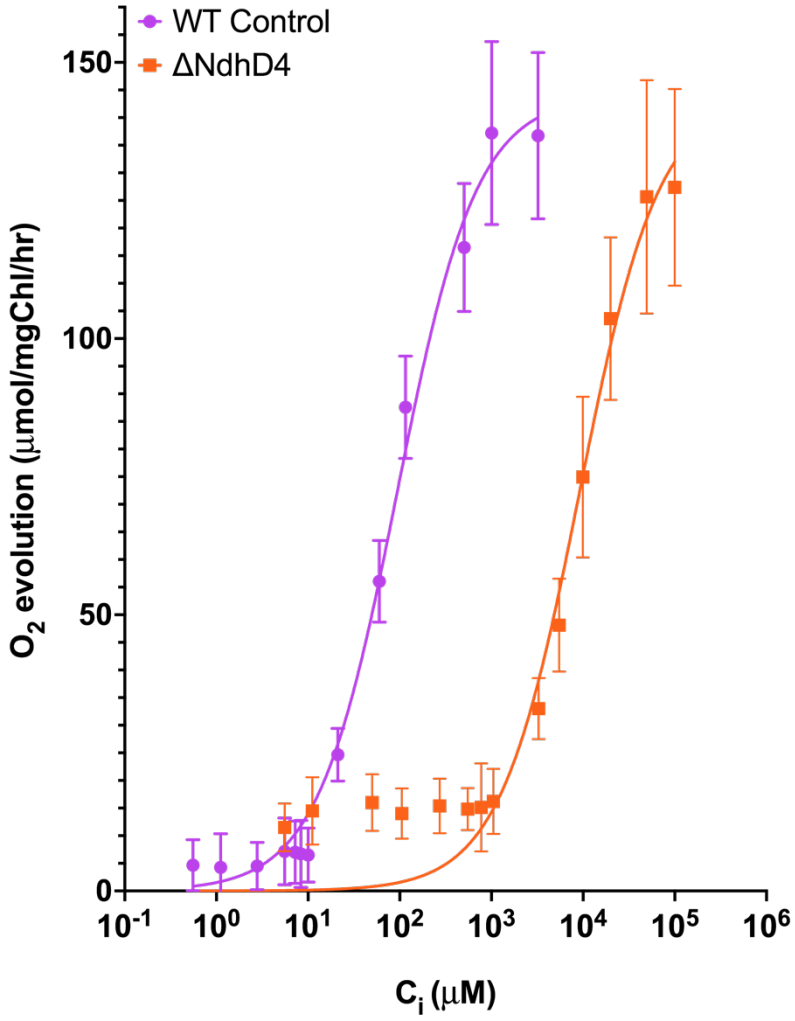

Figure 14. Assays for C_i uptake/Affinity measuring photosynthetic O_2 evolution rates in *Synechoccoccus* 7942 strains. Cells were grown in pH8 BG-11 at 5% CO_2 under 150 µE of light. Cells were harvested and resuspended to a chlorophyll concentration of 50µg/mL. Before assay, cells were washed and resuspended in BTP buffer. In BTP buffer, enough cells for 20µg of chlophyll resuspended in 2mL, was added to the measurement chamber. Cells were depleted of inorganic carbon. $KHCO_3$ was titrated into the measurement chamber in the presence of 25 µg of carbonic anhydrase. Traces consist of three biological replicates and three technical replicates (n=9). Error bars indicate standard deviation.

Cells were grown in standard conditions for NDH-1_4 complex experimentation, as described in the methods, for both strains. Both strains were assayed for three biological and three technical

replicates. When observing oxygen production of individual strains, there are three types of experiments that yield valuable information. These experiments include oxygen evolution probing for PSII quantification, maximal oxygen production rate, and cellular affinity for CO_2. The latter being calculate using a Michaelis-Menton curve fit.

Table 2: Photosynthetic O_2 evolution of NdhD4 mutant strains in response to C_i uptake. K_m describes the concentration of substrate at half the maximal rate of O2 evolution. V_{max} describes the maximal rate of O_2 evolution. N describes the sample size of three biological replicates and three technical replicates. Posassium bicarbonate was titrated in every minute for 15 minutes upon depletion of C_i. Values for each category are means. ±x indicates standard deviation.

Best Fit Value	ΔNdhD4	WT Control
K_m	9088 ± 1700	93.31 ± 10.9
V_{max}	144.0 ± 8.7	144.1 ± 4.6
N	9	9

To analyze the cell affinity to CO_2, $KHCO_3^-$ was added in incremental amounts to the sample in the presence of carbonic anhydrase. At pH7, this allows for the conversion of HCO_3^- to CO_2 without contribution of bicarbonate uptake via sodium symports. Experiments took placeover 15 minutes with an addition of $KHCO_3$ every minute. The O_2 production rates are calculations made by assessing of the slope of production 15 seconds after addition, spanning for 30 seconds. For enzyme kinetics calculations, titrations until the achievement of maximal O_2 production rate are included. Δ*ndhD4* is shown to have drastically decreased affinity towards CO_2 based off the K_m value of the curve fit. However, this strain exhibits a similar maximal rate compared to that of the wild type control (Figure 13 and Figure 14).

3.3 Δ*ndhD4* and Δ*ndhD4*/pSE4km_ *ndhD4* – PAM Fluorescence Trace

Pulse amplitude modulation (PAM) fluorometry was utilized to assess the fluorescence yield characteristics of individual strains. During charge separation in PSII of the light-dependent reactions, photoexcitation potential energy has three fates. If the energy is not used to perform photochemistry, then it dissipates either as heat or fluorescence. The PAM fluorimeter can measure this fluorescence by probing changes in fluorescence yield with a weak measuring beam of modulated red light that is only weakly actinic (1 µmole photons m^{-2}-sec^{-1}), followed by stronger (22 µmole photons m^{-2}-sec^{-1}) actinic light. The more fluorescence a strain produces, the less excitation energy is used in photochemistry. In these traces, cultures were prepared in standard conditions for NDH-1_4 complex experimentation as described in the methods. $KHCO_3^-$, along with carbonic anhydrase, were added to the samples before measurement assays began. The samples were then mixed thoroughly by pipetting up and down, but avoiding mixing with ambient air in the open optical cuvettes. The cells were then allowed to dark-adapt in the measurement chamber under the weak measuring beam for two minutes and thirty seconds. After the dark adaptation, the same set of triggered actinic light run was used for each measurement on both cultures. This triggered actinic light include three strong (~10000 µmole photons m^{-2}-sec^{-1}) multiple turnover flashes that last 300 msec each. These flashes allow for the saturation of all funtional PSII complexes and provide a reference value for the maximal fluorescence. These flashes occur before, after, and during the application of actinic measuring light. The actinic light in each experiment was applied to the sample for 5 minutes at 22 µmole photons m^{-2}-sec^{-1}. Each strain was measured in repetition for the biological replicates

(independent cultures of the strain) and three technical replicates (replicates of a given culture).

The difference in steady state fluorescence provides a benchmark for analyzing the photosynthetic health of an individual stain. This is evident as Δ*ndhD4* cells exhibits a higher steady state florescence compared to the WT cells indicating that the mutant is unable to assimilate the electrons produced by the light reaction. In addition, the plastoquinone pool in the WT control is more capable of oxidation after its reaction centers are activated by the actinic light. This information can be deduced from the distinct negative slope of the trace during actinic light in the WT Control (Figure 15). This is in stark contrast to the *ΔndhD4* strain which shows a slope closer to zero and at a much higher steady state level of fluorence yield. Additionally, the WT control exhibits a small post illumination rise after the actinic measuring light is shut off. This can be attributed to the ability of the strain to produce complex sugars, while the Δ*ndhD4* in contrast shows no post illumination rise, presumably due to its lack of ability to create sugars at an efficient rate.

Photochemical quenching values can be calculated from the following traces.

$$Q_P = (F_m - F_s) \,/\, (F_m - F_0)$$

F_m describes the max point of fluorescence during the period when the actinic measuring light is on, F_s describes the steady state fluorescence, which is the period of time during the actinic light application after the fluorescence reaches its max and before the light is turned off, F_0 describes the amount of fluorescence before any saturating flash or actinic light application.

This equation describes the photochemical quenching of a particular sample. In short, the larger the photochemical quenching value the more photochemical potential of the cell. In contrast,

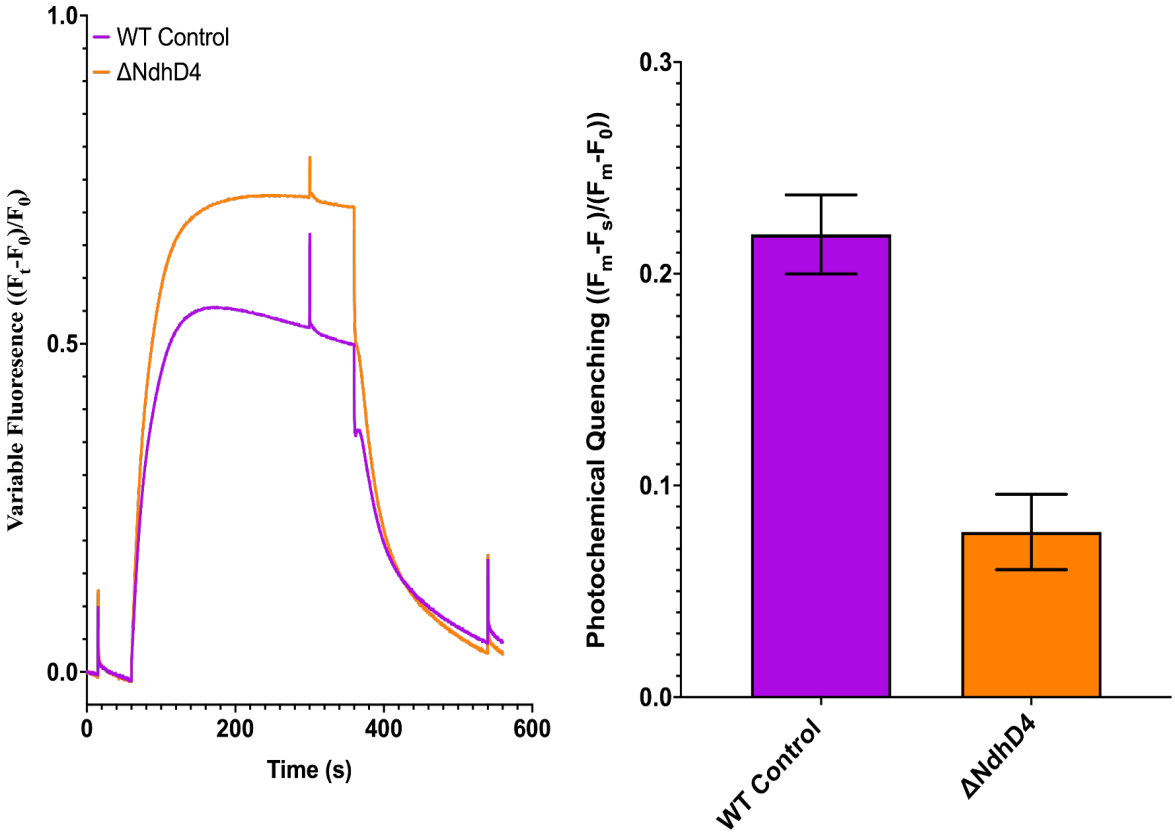

Figure 15. Fluorescence traces from PAM fluorometer measuring amount of chlorophyll fluorescence in *Synechococcus* 7942 Cells were grown in pH8 BG-11 at 5% CO_2 under 150 µE of light. Cells were harvested and resuspended to a chlorophyll concentration of 50µg/mL. Before assay, cells were washed and resuspended in BTP buffer. In BTP buffer, enough cells for 20µg of chlorophyll resuspended in 2mL, was added to the measurement chamber. Cells were allowed to dark adapt. Saturating flashes of light occurred 20, 300 and 540 seconds. Actinic measuring light at 22µE was applied starting at 60 seconds and lasting for five minutes (left). Photochemical Quenching (Qp) was calculated using the equation $(F_m - F_s) / (F_m - F_0)$. Chlorophyll quenching describes the over photosynthetic potential of a cell (right).

the lower the photochemical quenching of the cell the less photochemical potential of the cell. That being said, conclusions can be drawn regarding particular mutations based on how the photochemical quenching value compares to the wild type. Strains that have similar Q_p values as the WTcontrol do not have a damaged photochemical pathway and perform photosynthesis

relatively optimally. Compared to the WT control, Δ*ndhD4* has significantly lower Q_p, indicating that the removal of the NdhD4 antiporter-like subunit greatly effects the overall photochemical potential of the cell (Figure 15). In other words, ΔNdhD4 cells are less capable of using products made in the light independent and light dependent reactions. This leads to a backup of electrons through the light dependent reactions. This back up forces the potential energy created upon Chl excitation to be lost as fluorescence. In contrast the WT control, under NDH-1_4 probing conditions, uses its excited electrons form PSI and PSII much more efficiently, allowing said potential energy to be used to make CBB Cycle secondary products such as NADPH an not to be lost as flouresence. Thus, the strains that have lower photochemical potential have a hindered ability to photosynthesize most likely due to a limitation in the ability to fix CO_2. Because the mutations produce defects in the NDH-1 complexes associated with CO_2 uptake, lower photochemical potential is likely due to impaired CO_2 hydration activity by the mutant NDH-1 complexes.

CHAPTER IV

PHENOTIPIC ASSAYS FOR POINT MUTANT STRAINS

4.1 Identification of essential amino acid residues in NdhD4

Upon inspection and comparison of the WT control and Δ*ndhD4*, it was determined that the difference in phenotype across the various physiological assays warranted a more in-depth exploration of the functionality of the NdhD4 subunit. To do this, individual residues were selected that were hypothesized to be critical to the functionality of the complex and therefore the subunit as a whole. Mutant were selected based on homology modeling, multiple sequence alignments, and careful consideration of the complex itself with knowledge of Complex I in mind. Phenotypic assays for individual point mutations were assessed using the CO_2 affinity and PAM Florescence assays. Spot-growth assays were used initially to detect phenotypic vaiations in point mutant strains, but notable difference in autotrophic growth could not be detected between the point mutations and the knockout. Significant differences were detected using the far more sensitive, quantitative assays. For clarity and conceptualization purposes, the individual point mutations are displayed in two groups. One group consisits of data from point mutant strains H232Y and H332A. The other group consists of data from point mutant strains E137Q, E139Q, and K218E

4.2 CO_2 Uptake assays: H332A and H232Y

Cells were grown in standard conditions for NDH-1_4 complex experimentation as described in the methods. All strains were assayed for three biological and three technical replicates. When

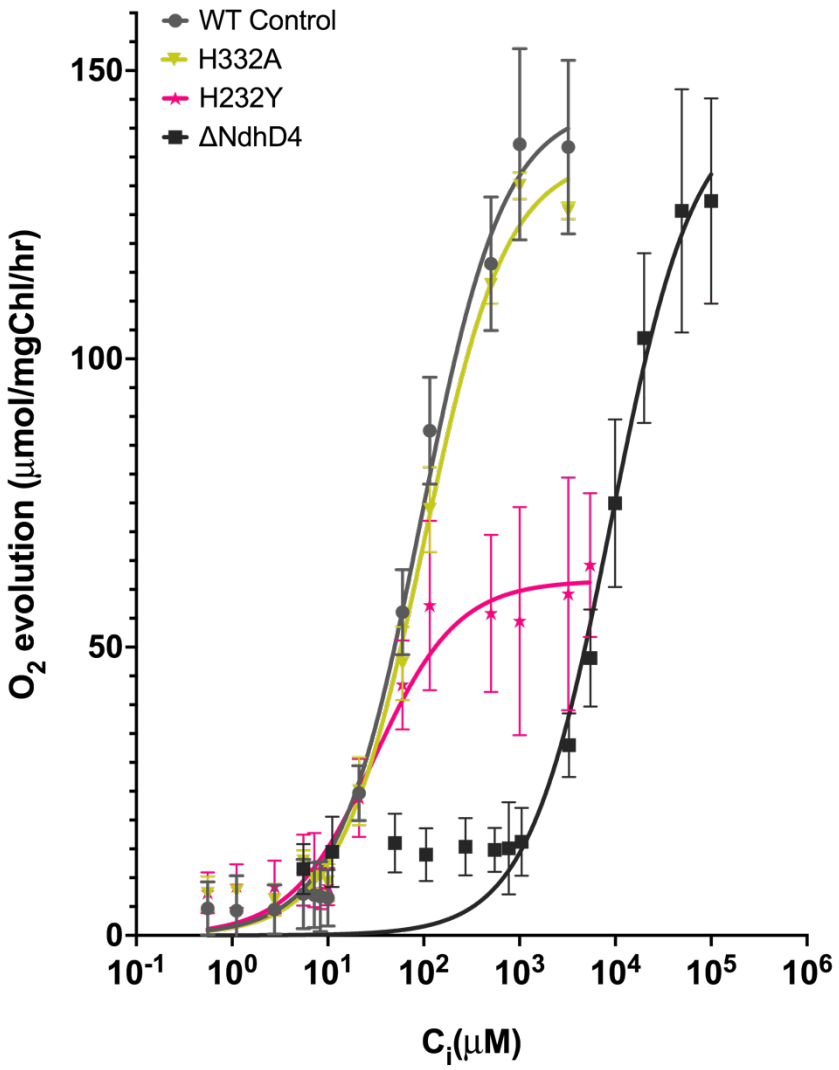

Figure 16. Assays for C_i uptake/Affinity measuring photosynthetic O_2 evolution rates in *Synechococcus* 7942 strains. Cells were grown in pH8 BG-11 at 5% CO_2 under 150 µE of light. Cells were harvested and resuspended to a chlorophyll concentration of 50µg/mL. Before assay, cells were washed and resuspended in BTP buffer. In BTP buffer, enough cells for 20µg of chlorophyll resuspended in 2mL, was added to the measurement chamber. Cells were depleted of inorganic carbon. $KHCO_3$ was titrated into the measurement chamber in the presence of 25 µg of carbonic anhydrase. Traces consist of three biological replicates and three technical replicates (n=9). Error bars indicate standard deviation.

observing oxygen production of individual strains, there are three types of experiments that yield valuable information. These experiments include oxygen evolution probing for PSII quantification, maximal oxygen production rate, and cellular affinity for CO_2. The latter being calculate using Michaelis-Menten curve fit. To analyze the cell affinity to CO_2, $KHCO_3$ was added in incremental amounts to the sample in the presence of carbonic anhydrase. This allows for the conversion of HCO_3^- to CO_2 without uptake of HCO_3^- by the sodium symports. Experiments took please over 15 minutes with an addition of $KHCO_3$ every minute. O_2 production rates are calculations of the slope of production 15 seconds after addition, spanning for 30 seconds. To assess the phenotype of the point mutants, both controls were used as a reference.

H233A exhibited an affinity and maximal rate akin to that of the WT Control (Figure 17, Table 2). H232Y, meanwhile, showed a significant decrease in the maximal rate of oxygen production compared to the knockout mutant and the WT control. However, H232Y displayed a similar affinity towards CO_2 as that of the WT control. This is a unique phenotype, considering the phenotype of both the WT Control strain and the Δ*ndhD4* strain.

4.3 Oxygen Production- Maximal Rates: H332A and H232Y

Upon investigation of the oxygen uptake characteristics of the individual mutants, a phenotype of differential maximal rates was discovered. This value was calculated after a long titration. To

confirm the result, an experiment that assessed just the maximal oxygen production rate of an individual strain was performed. Cells were treated the same as cells for NDH-1_4 complex analysis, but with difference in only the amount of HCO_3^- added. The cells were supplemented with saturating amounts of $KHCO_3$, in the presence of carbonic anhydrase, allowing for the analysis of the maximal possible rate the cell is capable of using its NDH-1_4 complex to assist in hydrating CO_2 and powering the Calvin cycle.

Table 3: Photosynthetic O_2 evolution of NdhD4 mutant strains in response to C_i uptake. K_m describes the concentration of substrate at half the maximal rate of O2 evolution. V_{max} describes the maximal rate of O_2 evolution. N describes the sample size of three biological replicates and three technical replicates. Posassium bicarbonate was titrated in every minute for 15 minutes upon depletion of C_i. Values for each category are means. ±x indicates standard deviation.

Best Fit Value	ΔNdhD4	WT Control	H332A	H232Y
K_m	9088 ± 1700	93.3 ± 10.9	98.7 ± 13.7	30.4 ± 7.1
V_{max}	144.0 ± 8.7	144.1 ± 4.6	135.2 ± 5.0	61.5 ± 3.7
N	9	9	9	9

Indeed, H232Y and H332A exhibited similar phenotypes, with respect to their maximal rate, as shown in the long titration experiments. With both the maximal rate experiment and the data gathered from the 15 minute affinity assay, it can be concluded that these maximal rates are a real phenotype (Table 2).

4.4 PAM florescence- H332A and H232Y

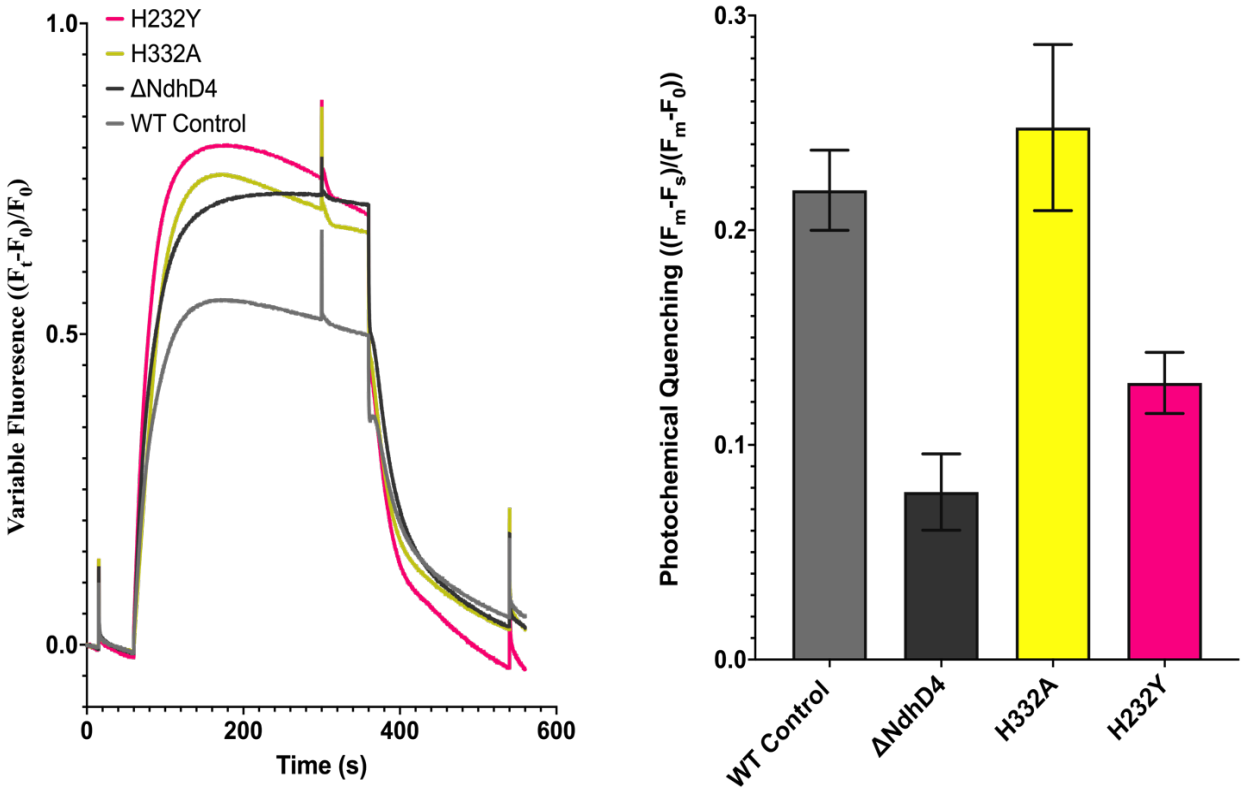

Figure 17. Fluorescence traces from PAM fluorometer measuring amount of chlorophyll fluorescence in *Synechococcus* 7942 Cells were grown in pH8 BG-11 at 5% CO_2 under 150 µE of light. Cells were harvested and resuspended to a chlorophyll concentration of 50µg/mL. Before assay, cells were washed and resuspended in BTP buffer. In BTP buffer, enough cells for 20µg of chlorophyll resuspended in 2mL, was added to the measurement chamber. Cells were allowed to dark adapt. Saturating flashes of light occurred 20, 300 and 540 seconds. Actinic measuring light at 22µE was applied starting at 60 seconds and lasting for five minutes (left). Photochemical Quenching (Qp) was calculated using the equation $(F_m - F_s)$ / $(F_m - F_0)$. Chlorophyll quenching describes the over photosynthetic potential of a cell (right).

Cells were grown under conditions for NDH-1$_4$ investigation. Before investigations cells were resuspended to 50 µg/ml of Chl. 5µg of Chl were used for experimental analysis. Cells were, again, washed and resuspended with bis-tris propane buffer (BTP). BTP buffer functions to drive off remaining inorganic carbon in the cell suspension. Cells were supplemented with carbonic anhydrase and $KHCO_3$ during data collections. The individual samples were probed using the

standard light sequence as used previously. H232Y and H332A both exhibit steady state fluorescence comparable to that of Δ*ndhD4*. However, there is also a distinct oxidation event exhibited over the span of the actinic light application. Which is not observed in Δ*ndhD4*. This oxidation phenotype is more comparable to that of the WT Control. Other than those two distinct phenotypes, everything else about the fluorescence trace is as expected.

The Q_p of H332A and H232Y yield some unexpected and inconsistent results. When comparing Q_p to trends in the general fluorescence traces, there are inconsistencies with the H332A mutant. While the steady state florescence, and the trend of steady state most resemble the phenotype of Δ*ndhD4*, the Q_p of the strain is not stastically different than the WT control. H332 yields more consistent results. Similar to fluorescence traces the, Q_p is drastically lower than the WT control, and comparable to Δ*ndhD4*.

4.5 CO_2 Uptake assays: E139Q, K218E, E137Q

Table 4: Photosynthetic O_2 evolution of NdhD4 mutant strains in response to C_i uptake. K_m describes the concentration of substrate at half the maximal rate of O2 evolution. V_{max} describes the maximal rate of O_2 evolution. N describes the sample size of three biological replicates and three technical replicates. Posassium bicarbonate was titrated in every minute for 15 minutes upon depletion of C_i. Values for each category are means. ±x indicates standard deviation.

Best Fit Value	ΔNdhD4	WT Control	E137Q	E139Q	K218E
K_m	9088 ± 1700	93.3 ± 10.9	31.3 ± 6.6	75.1 ± 11.1	39.1 ± 11.0
V_{max}	144.0 ± 8.0	144.1 ± 4.6	87.3 ± 7.0	162.8 ± 6.6	76.8 ± 6.3
N	9	9	9	9	9

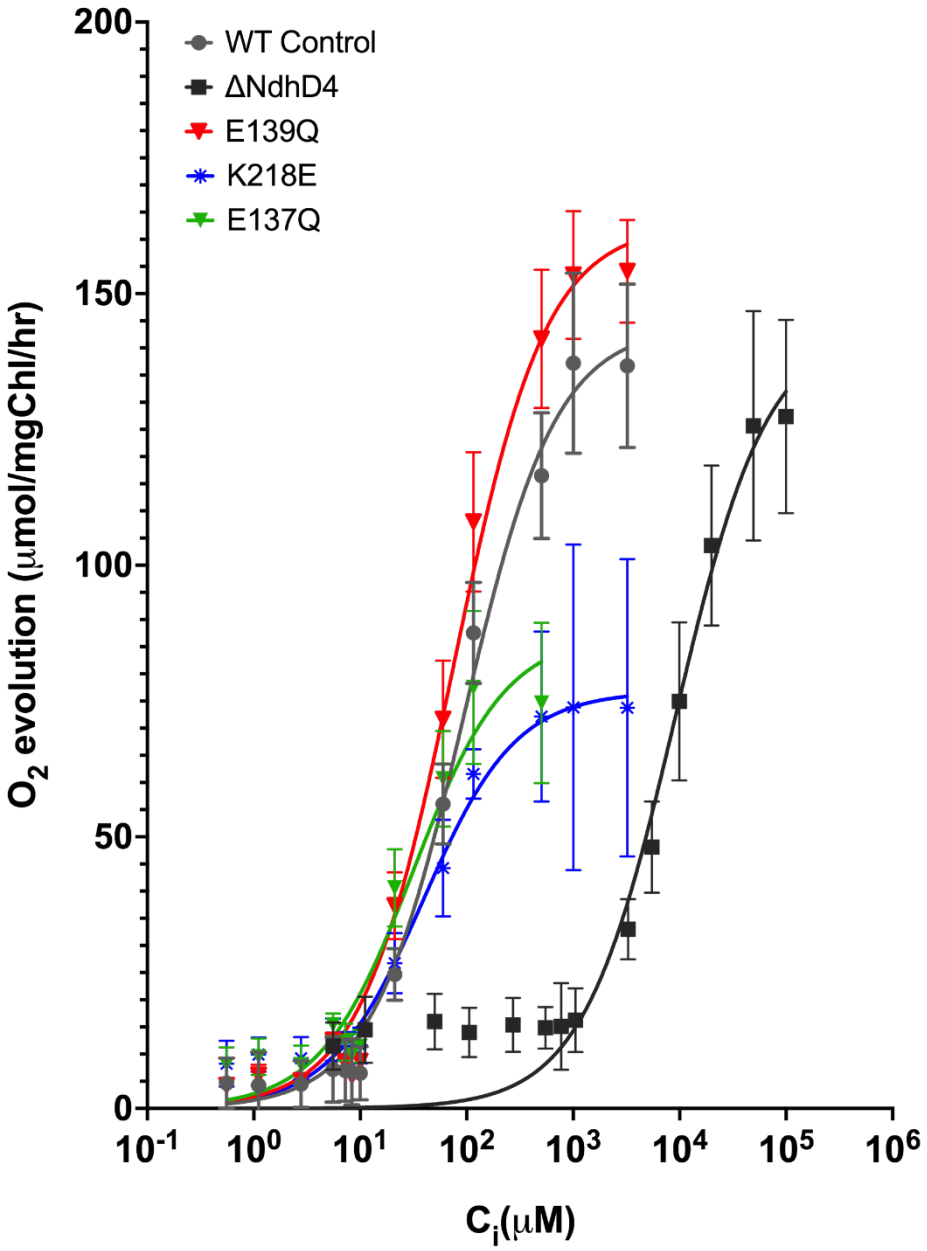

Figure 18. Assays for C_i uptake/Affinity measuring photosynthetic O_2 evolution rates in *Synechococcus* 7942 strains. Cells were grown in pH8 BG-11 at 5% CO_2 under 150 µE of light. Cells were harvested and resuspended to a chlorophyll concentration of 50µg/mL. Before assay, cells were washed and resuspended in BTP buffer. In BTP buffer, enough cells for 20µg of chlorophyll resuspended in 2mL, was added to the measurement chamber. Cells were depleted of inorganic carbon. $KHCO_3$ was titrated into the measurement chamber in the presence of 25 µg of carbonic anhydrase. Traces consist of three biological replicates and three technical replicates (n=9). Error bars indicate standard deviation.

Cells used for CO_2 uptake assays were processed in the exact same way as previously stated for other mutants and controls. The same titration method with carbonic anhydrase was used to analyze the CO_2 uptake ability of the cells. That being said mutants K218E and E137Q, like that of previous point mutant phenotypes, exhibits a similar affinity for CO_2 but a significantly smaller maximal rate to that of both controls. This is in contrast to the phenotype of that of E139Q. E139Q has the same high affinity phenotype compared to that of the WT control, but a larger maximal rate, contrasting from the phenotype of other point mutations.

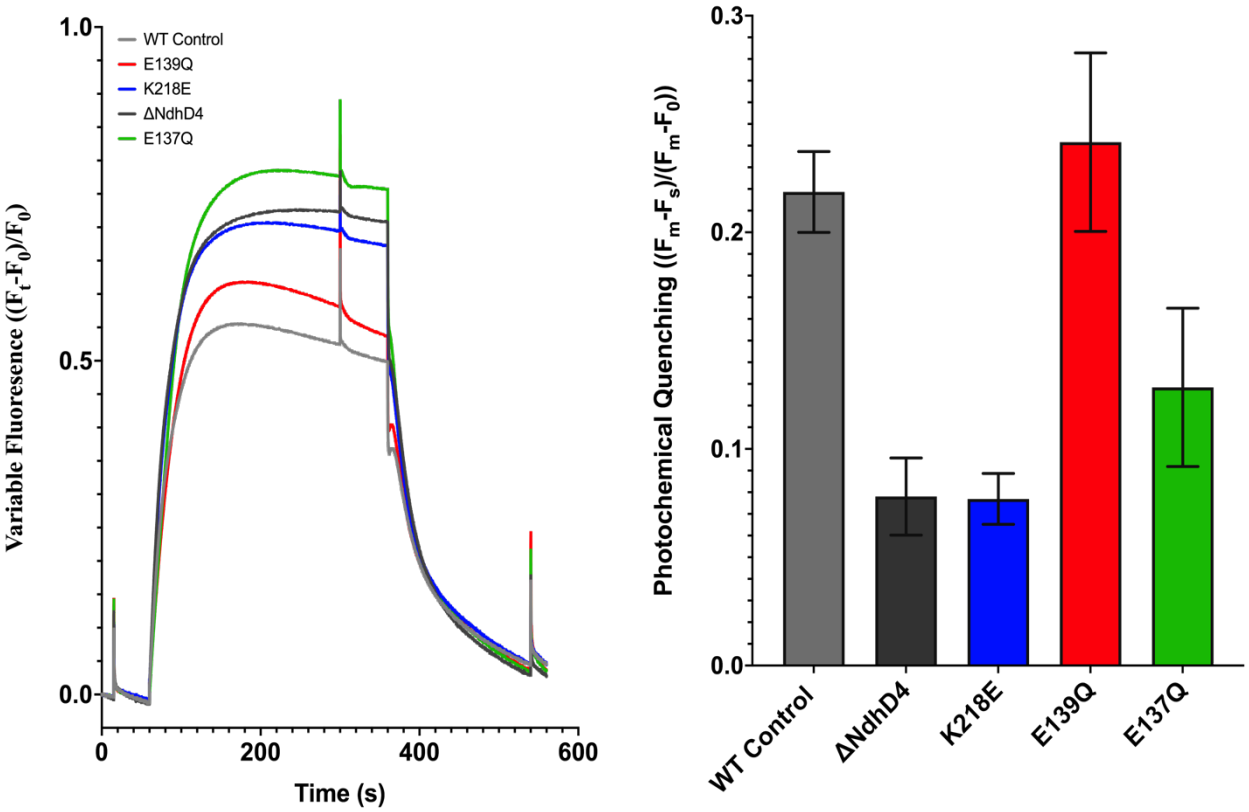

Figure 19. Fluorescence traces from PAM fluorometer measuring amount of chlorophyll fluorescence in *Synechococcus* 7942 Cells were grown in pH8 BG-11 at 5% CO_2 under 150 µE of light. Cells were harvested and resuspended to a chlorophyll concentration of 50µg/mL. Before assay, cells were washed and resuspended in BTP buffer. In BTP buffer, enough cells for 20µg of chlorophyll resuspended in 2mL, was added to the measurement chamber. Cells were allowed to dark adapt. Saturating flashes of light occurred 20, 300 and 540 seconds. Actinic measuring light at 22uE was applied starting at 60 seconds and lasting for five

4.6 PAM Fluorescence: E139Q, K218E, E137Q

Cells used for PAM florescence experiments were processed in the same way as previously stated for other mutants and controls. The same method for CO_2 depletion and readition were used. PAM fluorescence phenotypes for E139Q, K218E, and E137Q parallel to the phenotypes that were observed in the CO_2 uptake experiments. K218E and E137Q exhibited a similar Chl florescence trace to that of Δ*ndhD4*. It has a relatively high steady state fluorescence with a rate of oxidation similar to that of Δ*ndhD4*, meaning that there is relatively little oxidation over the duration of the actinic light application. Meanwhile, E139Q possess a trace more in line with the florescence trace of the WT control, both in the steady state fluorescence and the oxidation characteristics.

The Q_p of these mutants align with the results from experiments proceeding. K218E and E137Q have a lower Q_p, comparable to that of Δ*ndhD4*. E139Q has a Q_p similar to that of WT Control.

CHAPTER V

DISCUSSION

The CO_2 hydrating ability of S7942 is essential for the cell to perform photosynthesis, create complex carbohydrates, and produce biomass. While it is known that cyanobacteria are capable of performing photosynthesis efficiently largely due to the CO_2 hydrating ability of its NDH-$1_{3/4}$ complexes, much is still unknown about the functionality of these complexes (Burnap et al., 2015; Long et al., 2016; Price et al., 2008). Previous research has shown a few important attributes of these complexes (Bernát, Appel, Ogawa, & Rögner, 2011; Mi et al., 1992; Ohkawa, Pakrasi, et al., 2000; Ohkawa, Price, et al., 2000; Shibata et al., 2001a). First, the structure has been resolved allowing for the elucidation of the carbonic anhydrase like activity of the complex. Additionally, the complexes have been shown to be structurally and functionally similar to that of respiratory complex 1 (Schuller et al., 2020). What is still unknown, is how these two reactions (redox/carbonic anhydrase) are coupled and proceed in an efficient manner. From previous research done on complex 1, it is known that the membrane-bound subunits are responsible for proton-pumping in an effort to establish a proton gradient for ATP synthase (Gutiérrez-Fernández et al., 2020; Parey et al., 2021; Sato, Sinha, Torres-Bacete, Matsuno-Yagi, & Yagi, 2013; Sharma et al., 2009). It is thought that the CO_2 hydrating reaction occurring in NDH-$1_{4,3}$ complexes, use the ability of this complex to pump protons in order to energize the CO_2 hydration reaction (Artier, Holland, Miller, Zhang, & Burnap, 2018; Artier et al., 2022; Miller, Vaughn, & Burnap, 2021; Schuller et al., 2020).

This includes the NdhD4 subunit. Gene deletions and mutations made in this study elucidates that the NdhD4 protein is in some way, critical to the function of the protein complex.

The general hypothesis guiding this research is that proton pumping involving the NdhD4 subunit is involved in the CO_2 hydration activity of the NDH-1_4 complex. By using a strain that lacks activity of both the NDH-1_3 and NDH-1_4 complexes and with the ability to engineer strains that restore the NDH-1_4 complexes with altered forms of the NdhD4 protein, we can begin to examine the structure-function relationships of the NdhD4 protein. To better understand the functionality of NdhD4, it is essential to look at each individual mutation and how it may function with respect to respiratory complex I. By examining the literature, using homology relationships of conserved amino acids, we can target specific residues likely to participate in proton pumping. We can also consider current hypotheses regarding the mechanism of Complex I proton pumping, which is discussed as trap/gate mechanism (V. R. Kaila, Wikstrom, & Hummer, 2014; V. R. I. Kaila, 2018; Mühlbauer et al., 2020; Saura & Kaila, 2019) as described in the introduction. Here we tested some of the residues proposed to be involved in this water wire/charge relay trap and gate mechanism used to shuttle protons away from the active site of the CO_2 hydration reaction occurring in in CupB subunit. In any event and regardless of the hypothesized details, the residues targeted are homologous to residues in the *E. coli* protein that have been definitively tested and produce impacts on proton pumping (Sato et al., 2013; Sato et al., 2014).

When the *ndhD4* gene is completely deleted and the protein can no longer be expressed, we see a phenotype similar to that of a deletion of the CupB *cupB* gene is observed. This is indicative of a complete loss of function and minimally the dissociation of, at least, the

remaining parts of the CO_2 hydrating portion of the complex, CupB and NdhF4. Without the insert of this subunit in the membrane, it appears that the rest of the protein complex cannot assemble and accumulate in the membrane correctly, indication that the NdhD4 subunit is essential, structurally, to the protein complex. However, I was not able to directly test the accumulation of these proteins since the antibodies we need are still being developed. Alternatively, we will analyze the accumulation using mass spectroscopic methods (Artier et al., 2022).

Analysis of the deletion mutant, Δ*ndhD4*, does not give us clues about the detailed functionality of the NdhD4 subunit. Again, to investigate this, point mutations were constructed and analyzed at residues that were hypothesized to be critical to the complex's functional mechanism. These mutations consist of charged, acidic or basic, resides along the hypothesized water wire, as well as residues that may be along a potential proton pathway throughout the top half of the subunit, to this charged gating mechanism.

Residues along the hypothesized charge relay system include E139, K218, and E137. To analyze if these residues are essential for the charge relay system, we mutated them to opposite charged mutations, based upon previous studies with *E. coli,* which disrupted function, but allowed accumulation of the protein product in the homologous system (Sato et al., 2013; Sato et al., 2014). Mutations of these residues should, theoretically, upset the delicate balance of ordered opposite charges, disallowing the precise pKa shifts to proceed up and down the membrane-bound proteins. If the pKa cannot change within these mutants then the gating mechanism and release of protons cannot occur. Interestingly we see that K218E and E137Q have a distinct effect on the CO_2 hydrating ability of the cell. This elucidates that these residues

are in fact somewhat essential for optimal CO_2 hydration. Supporting our hypothesis that they are part of the complexe's charge relay system.

The peculiar part of the results however is the phenotype that they produce, particularly with the CO_2 affinity experiments. Initially we expected that mutated critical residues would produce a phonotype that differs in the CO_2 affinity of the cell, i.e. the K_m value of the Michaelis-Menten curve describing the enzyme kinetics of the reaction. This, however, was not the case. Instead, we observed a decrease in the overall rate of oxygen production.

We think that this is particularly due to the inability of the residue of interest to dissociate and interact with its neighboring residue upon a change in pKa. In summary, when a residue of interest is changed to one of an opposite charge, its neighboring residue will at some point dissociate from its current state and attempt to interact with the mutated residue. However, the residues charge characteristics would no longer permit for an interaction, allowing the particular amino acid to swing freely on one side and interact only on the opposite (Fig. 4). While not initially effecting the enzyme kinetics at the active site, it is thought that this inability to remove protons optimally backs up the process, eventually affecting the overall ability of the cell to produce HCO_3^-. This in turn affects the ability of the cell to carbonate it cytoplasm and hydrate CO_2. This basic principle can be applied to both the K218E mutant and the E137Q mutant.

In addition to this, we investigated particular histidine residues that we hypothesize could be part of the pathway towards the proposed water wire/charge relay system. It is understood that histidine residues are of particular interest because of their ability to transfer protons, making them particularly interesting residues to target in order to probe a potential proton

pathway. The residues we chose were H232 and H332, mutated to a tyrosine and an alanine respectively. Only H232Y yielded significantly different results compared to both the positive and negative controls. H232Y interestingly yielded similar phenotypes to those of the mutations along the water wire. We think that the phenotypes are similar due to a similar effect on the active site of the Cup protein. If the ability for the proton to be shuttled to the charge relay mechanism, then the phenotype would potential be affected in a similar way. Initially the affinity is not affected, but the rate is affected after the inevitable accumulation of produced protons. When protons are backed up, the reactions become less energetic, trending towards the production of CO_2 and H_2O, ultimately reducing the amount of bicarbonate produced.

CHAPTER VI

SUMMARY

The current climate crisis and increasing atmospheric CO_2 concentrations is more of a relevant problem than it ever has. Mitigation of atmospheric CO_2 is a complex challenge with no simple solution. However, investigation into the cyanobacterial carbon concentrating mechanism, particularly the CO_2 hydrating complexes, my give clues regarding potential CO_2 remediation solutions.

In an effort to constantly occupy the active site of RuBisCO, cyonabacterial employs the super carbonating abilities of its NDH-$1_{4,3}$ CO_2 hydra ting complexes. I. We hypothesized that this super carbonation phenomenon is made possible through the biochemical coupling of both the redox reactions and the CO_2 hydration reaction. To drive the CO_2 hydration reaction far from equilibrium and favor the production of our non-permeable bicarbonate, cyanobacteria rely on the proton pumping (product removal) of the membrane-bound antiporter-like subunits of its NDH-1_4 complex. This is made possible through the activation of a charge/gate mechanism in the membrane bound subunits that is activated from redox reactions occurring opposite of CupB in the peripheral membrane arm. The redox ractions occurring trigger both a conformational and electrostatic change in a series of charged ammino acids near the center of these membrane bound proteins.

This change in charge to ammino acid residues allow for differential interactions between each other and with water. This change effects how protons are allowed to move through the subunits, mediated by water molecule, which allow for rapid proton translocation.

In addition we hypothesized that the NdhD4 protein subunit, in particular, is essential for this proton translocation, aiding in the energized CO_2 hydration reaction occurring in CupB. We also hypothesize that the NdhD4 subunit contains and require these charged amino acids that are part of the water wire/charge relay system. We hypothesized that these residues are critical for the proton pumping ability of the subunit, and therefore the CO_2 hydrating ability of the complex.

When the *ndhD4* gene was deleted, the CO_2 hydrating ability of the NDH-1_4 complex was abolished. This is presumabley due to the complete dissociation of CO_2 hydrating side of the NDH-1_4 complex. This was evident from the substantial decrease in steady state fluoresence, decrease in $Q_{p.}$ Five residues in NdhD4 were hypothesized to be critical based in information gathered from the highly studied Complex I of the respiratory chain. These residues were mutated in a manner that would, hopefully, result in a loss of function.

Suprisingly, the mutated residues exhibited a phenotype, in the CO_2 uptake assay that was different from the knockout. Three of the five mutants were shown to impact the photype of the cell and therefore the funconality of the NDH-1_4 complex. These mutatnts were E137Q, K218E, and H232Y. This means that the residues E137, K218, and H232 are, plausibly, critical for the proton pumping ability of the complex. These critical residues, when mutated, exhibited a decrease in maximal O_2 production rate rather than a decrease in CO_2 affinity. At the same time,

these mutants showed a drastically decreased Q_p value compared to the WT control and mutants of little to no significance (E139Q and H332A).

These outlined phenotypes in selected mutants support our hypotheses regarding the proton pumping of NdhD4 as well as the mechanism of said proton pumping.

REFERENCES

Artier, J., Holland, S. C., Miller, N. T., Zhang, M., & Burnap, R. L. (2018). Synthetic DNA system for structure-function studies of the high affinity CO(2) uptake NDH-1(3) protein complex in cyanobacteria. *Biochimica et biophysica acta. Bioenergetics*, S0005-2728(0018)30175-30170. doi:10.1016/j.bbabio.2018.06.015

Artier, J., Walker, R. M., Miller, N. T., Zhang, M., Price, G. D., & Burnap, R. L. (2022). Modeling and mutagenesis of amino acid residues critical for CO2 hydration by specialized NDH-1 complexes in cyanobacteria. *Biochimica et Biophysica Acta (BBA) - Bioenergetics, 1863*(1), 148503. doi:https://doi.org/10.1016/j.bbabio.2021.148503

Badger, M. R. (1980). Kinetic properties of ribulose 1,5-bisphosphate carboxylase/oxygenase from Anabaena variabilis. *Archives of Biochemistry and Biophysics, 201*(1), 247-254. doi:https://doi.org/10.1016/0003-9861(80)90509-3

Bernát, G., Appel, J., Ogawa, T., & Rögner, M. (2011). Distinct Roles of Multiple NDH-1 Complexes in the Cyanobacterial Electron Transport Network as Revealed by Kinetic Analysis of P700⁺ Reduction in Various ndh-Deficient Mutants of Synechocystis sp. Strain PCC6803. *Journal of bacteriology, 193*(1), 292-295. doi:doi:10.1128/JB.00984-10

Blankenship, R. E. (2010). Early Evolution of Photosynthesis. *Plant Physiology, 154*(2), 434-438. doi:10.1104/pp.110.161687

Blankenship, R. E. (2021). *Molecular Mechanisms of Photosynthesis*: Wiley.

Burnap, R. L., Hagemann, M., & Kaplan, A. (2015). Regulation of CO2 Concentrating Mechanism in Cyanobacteria. *Life (Basel, Switzerland), 5*(1), 348-371. doi:10.3390/life5010348

Chen, Y., Taton, A., Go, M., London, R. E., Pieper, L. M., Golden, S. S., & Golden, J. W. (2016). Self-replicating shuttle vectors based on pANS, a small endogenous plasmid of the unicellular cyanobacterium Synechococcus elongatus PCC 7942. *Microbiology, 162*(12), 2029-2041. doi:10.1099/mic.0.000377

Ding, X., Matsumoto, T., Gena, P., Liu, C., Pellegrini-Calace, M., Zhong, S., . . . Calamita, G. (2013). Water and CO_2 permeability of SsAqpZ, the cyanobacterium Synechococcus sp. PCC7942 aquaporin. *Biol Cell, 105*(3), 118-128. doi:10.1111/boc.201200057

Golbeck, J. (2004). Photosynthetic reaction centers: So little time, so much to do. *Biophysics Textbook Online, http://www. biophysics. org/education/golbeck. pdf*.

Gutiérrez-Fernández, J., Kaszuba, K., Minhas, G. S., Baradaran, R., Tambalo, M., Gallagher, D. T., & Sazanov, L. A. (2020). Key role of quinone in the mechanism of respiratory complex I. *Nature Communications, 11*(1), 4135. doi:10.1038/s41467-020-17957-0

Jiang, Y., Qian, F., Yang, J., Liu, Y., Dong, F., Xu, C., . . . Yang, S. (2017). CRISPR-Cpf1 assisted genome editing of Corynebacterium glutamicum. *Nature Communications, 8*(1), 15179. doi:10.1038/ncomms15179

Kaila, V. R., Wikstrom, M., & Hummer, G. (2014). Electrostatics, hydration, and proton transfer dynamics in the membrane domain of respiratory complex I. *Proc Natl Acad Sci U S A, 111*(19), 6988-6993. doi:10.1073/pnas.1319156111

Kaila, V. R. I. (2018). Long-range proton-coupled electron transfer in biological energy conversion: towards mechanistic understanding of respiratory complex I. *J R Soc Interface, 15*(141). doi:10.1098/rsif.2017.0916

Long, B. M., Rae, B. D., Rolland, V., Förster, B., & Price, G. D. (2016). Cyanobacterial CO2-concentrating mechanism components: function and prospects for plant metabolic engineering. *Current Opinion in Plant Biology, 31*, 1-8. doi:https://doi.org/10.1016/j.pbi.2016.03.002

Mi, H., Endo, T., Schreiber, U., Ogawa, T., & Asada, K. (1992). Electron Donation from Cyclic and Respiratory Flows to the Photosynthetic Intersystem Chain is Mediated by Pyridine Nucleotide Dehydrogenase in the Cyanobacterium Synechocystis PCC 6803. *Plant and Cell Physiology, 33*(8), 1233-1237. doi:10.1093/oxfordjournals.pcp.a078378

Miller, N. T., Vaughn, M. D., & Burnap, R. L. (2021). Electron flow through NDH-1 complexes is the major driver of cyclic electron flow-dependent proton pumping in cyanobacteria. *Biochim Biophys Acta Bioenerg, 1862*(3), 148354. doi:10.1016/j.bbabio.2020.148354

Mühlbauer, M. E., Saura, P., Nuber, F., Di Luca, A., Friedrich, T., & Kaila, V. R. I. (2020). Water-gated proton transfer dynamics in respiratory complex I. *J Am Chem Soc, 142*(32), 13718-13728. doi:10.1021/jacs.0c02789

Mullineaux, C. W. (2014). Co-existence of photosynthetic and respiratory activities in cyanobacterial thylakoid membranes. *Biochim Biophys Acta, 1837*(4), 503-511. doi:10.1016/j.bbabio.2013.11.017

Nakamaru-Ogiso, E., Kao, M.-C., Chen, H., Sinha, S. C., Yagi, T., & Ohnishi, T. (2010). The Membrane Subunit NuoL(ND5) Is Involved in the Indirect Proton Pumping Mechanism of Escherichia coli Complex I *Journal of Biological Chemistry, 285*(50), 39070-39078. doi:10.1074/jbc.M110.157826

Nelson, N., & Yocum, C. F. (2006). Structure and function of photosystems I and II. *Annu Rev Plant Biol, 57*, 521-565. doi:10.1146/annurev.arplant.57.032905.105350

Niu, T.-C., Lin, G.-M., Xie, L.-R., Wang, Z.-Q., Xing, W.-Y., Zhang, J.-Y., & Zhang, C.-C. (2019). Expanding the potential of CRISPR-Cpf1-based Genome editing technology in the cyanobacterium Anabaena PCC 7120. *ACS Synthetic Biology, 8*(1), 170-180. doi:10.1021/acssynbio.8b00437

Ohashi, Y., Shi, W., Takatani, N., Aichi, M., Maeda, S.-i., Watanabe, S., . . . Omata, T. (2011). Regulation of nitrate assimilation in cyanobacteria. *Journal of Experimental Botany, 62*(4), 1411-1424. doi:10.1093/jxb/erq427

Ohkawa, H., Pakrasi, H. B., & Ogawa, T. (2000). Two types of functionally distinct NAD(P)H dehydrogenases in Synechocystis sp. strain PCC6803. *The Journal of biological chemistry, 275*(41), 31630-31634. doi:10.1074/jbc.M003706200

Ohkawa, H., Price, G. D., Badger, M. R., & Ogawa, T. (2000). Mutation of ndh genes leads to inhibition of CO(2) uptake rather than HCO(3)(-) uptake in Synechocystis sp. strain PCC 6803. *Journal of bacteriology, 182*(9), 2591-2596. doi:10.1128/jb.182.9.2591-2596.2000

Parey, K., Lasham, J., Mills, D. J., Djurabekova, A., Haapanen, O., Yoga, E. G., . . . Zickermann, V. (2021). High-resolution structure and dynamics of mitochondrial complex I—Insights into the proton pumping mechanism. *Science Advances, 7*(46), eabj3221. doi:doi:10.1126/sciadv.abj3221

Price, G. D. (2011). Inorganic carbon transporters of the cyanobacterial CO_2 concentrating mechanism. *Photosynthesis Research, 109*(1-3), 47-57. doi:10.1007/s11120-010-9608-y

Price, G. D., Badger, M. R., Woodger, F. J., & Long, B. M. (2008). Advances in understanding the cyanobacterial CO2-concentrating-mechanism (CCM): functional components, Ci transporters, diversity, genetic regulation and prospects for engineering into plants. *Journal of experimental botany, 59*(7), 1441-1461. doi:10.1093/jxb/erm112

Price, G. D., Coleman, J. R., & Badger, M. R. (1992). Association of Carbonic Anhydrase Activity with Carboxysomes Isolated from the Cyanobacterium Synechococcus PCC7942. *Plant Physiology, 100*(2), 784-793. doi:10.1104/pp.100.2.784

Price, G. D., Woodger, F. J., Badger, M. R., Howitt, S. M., & Tucker, L. (2004). Identification of a SulP-type bicarbonate transporter in marine cyanobacteria. *Proceedings of the National Academy of Sciences, 101*(52), 18228-18233. doi:10.1073/pnas.0405211101

Sambrook, J., Fritsch, E. F., and Maniatis, T. (1989). *Molecular cloning: A laboratory manual* (2 ed.). Cold Spring Harbor, New York: Cold Spring Harbor Laboratory.

Sato, M., Sinha, P. K., Torres-Bacete, J., Matsuno-Yagi, A., & Yagi, T. (2013). Energy transducing roles of antiporter-like subunits in Escherichia coli NDH-1 with main focus on subunit NuoN (ND2). *The Journal of biological chemistry, 288*(34), 24705-24716. doi:10.1074/jbc.M113.482968

Sato, M., Torres-Bacete, J., Sinha, P. K., Matsuno-Yagi, A., & Yagi, T. (2014). Essential regions in the membrane domain of bacterial complex I (NDH-1): the machinery for proton translocation. *J Bioenerg Biomembr, 46*(4), 279-287. doi:10.1007/s10863-014-9558-8

Saura, P., & Kaila, V. R. I. (2019). Molecular dynamics and structural models of the cyanobacterial NDH-1 complex. *Biochim Biophys Acta Bioenerg, 1860*(3), 201-208. doi:10.1016/j.bbabio.2018.11.010

Schuller, J. M., Saura, P., Thiemann, J., Schuller, S. K., Gamiz-Hernandez, A. P., Kurisu, G., . . . Kaila, V. R. I. (2020). Redox-coupled proton pumping drives carbon concentration in the photosynthetic complex I. *Nature Communications, 11*(1), 494. doi:10.1038/s41467-020-14347-4

Sharma, L. K., Lu, J., & Bai, Y. (2009). Mitochondrial respiratory complex I: structure, function and implication in human diseases. *Curr Med Chem, 16*(10), 1266-1277. doi:10.2174/092986709787846578

Shibata, M., Ohkawa, H., Kaneko, T., Fukuzawa, H., Tabata, S., Kaplan, A., & Ogawa, T. (2001a). Distinct constitutive and low-CO2-induced CO2 uptake systems in cyanobacteria: genes involved and their phylogenetic relationship with homologous genes in other organisms. *Proceedings of the National Academy of Sciences of the United States of America, 98*(20), 11789-11794. doi:10.1073/pnas.191258298

Shibata, M., Ohkawa, H., Kaneko, T., Fukuzawa, H., Tabata, S., Kaplan, A., & Ogawa, T. (2001b). Distinct constitutive and low-CO_2-induced CO_2 uptake systems in cyanobacteria: genes involved and their phylogenetic relationship with homologous genes in other organisms. *Proc Natl Acad Sci U S A, 98*(20), 11789-11794. Retrieved from http://www.ncbi.nlm.nih.gov/htbin-post/Entrez/query?db=m&form=6&dopt=r&uid=11562454

http://www.pnas.org/cgi/content/full/98/20/11789

http://www.pnas.org/cgi/content/abstract/98/20/11789

Tabita, F. R., Satagopan, S., Hanson, T. E., Kreel, N. E., & Scott, S. S. (2008). Distinct form I, II, III, and IV Rubisco proteins from the three kingdoms of life provide clues about Rubisco evolution and structure/function relationships. *Journal of experimental botany, 59*(7), 1515-1524. doi:10.1093/jxb/erm361

Torres-Bacete, J., Nakamaru-Ogiso, E., Matsuno-Yagi, A., & Yagi, T. (2007). Characterization of the NuoM (ND4) subunit in Escherichia coli NDH-1: conserved charged residues essential for energy-coupled activities. *J Biol Chem, 282*(51), 36914-36922. doi:10.1074/jbc.M707855200

Ungerer, J., & Pakrasi, H. B. (2016). Cpf1 Is A Versatile Tool for CRISPR Genome Editing Across Diverse Species of Cyanobacteria. *Scientific Reports, 6*, 39681. doi:10.1038/srep39681

Wilson, J. E. (2003). Isozymes of mammalian hexokinase: structure, subcellular localization and metabolic function. *Journal of Experimental Biology, 206*(12), 2049-2057. doi:10.1242/jeb.00241

APPENDICES

Photosystem II Quantification Analysis

To insure that point mutations are effecting the functionality of the CO_2 hydrating ability of the NDH-1_4 complex, it is essential to insure that the phonotype is not due to a decrease of cellular photosystem II content. For this experiment, the artificial electron acceptor system composed of 2,6-Dichloro-1,4-benzoquinone (DCBQ) and ferricyanide (FeCN) is added to cells to intercept electrons directly from photosystem II. These additions are made in standard BG-11 media in the oxygen electrode chamber. The DCBQ and FeCN combination allows for the electron pathway in the light dependent reactions to function independently of the water splitting reaction. DCBQ and FeCN saturate the electron transport chain, allowing for the quantification of photosystem, as they become the initial rate limiting variable in the photosynthetic reaction chain, not water splitting. This will allow a comparative analysis to be done for the controls/ mutants, to ensure that any phenotype observed is not due to an underlying lack of photosystems. To analyze this, the maximal rate of oxygen production is assessed. Cells are harvested and resuspended to a concentration of 50µg/ml Chl. They are then diluted to a concentration of 5µg/ml in the cuvette. In the dark, cells are supplemented with DCBQ and FCN. The light is then turned on to a saturating level and the oxygen production rate is harvested.

This is done with all controls and mutants and the maximal rates of each is compared to the maximal rate of its counterpart maximal rate when supplemented with inorganic carbon. If the maximal rate of the cells supplemented with DCBQ and FCN is lower than the maximal rate of cells of the same strain but supplemented with inorganic carbon, then the phenotype can be attributed to a lack of photosystem II.

For each strain and WT control, we see that the maximal rate of each strain, when supplemented with inorganic carbon, is much lower than the maximal rate than that with the DCBQ.

Proteomic Evaluation

Further work needs to be completed to assess each strains ability to accumulate the NdhD4 protein in its membrane. Using the knockout and the wild-type S7942 as a comparison, we want to perfrom immuneoblots of membrane fractions with antibody designed against the hydrophilic domain regions of the NdhD4 protein. Assessing the relative degrees of NdhD4 protein accumulation will allow us to better draw conclusion about the source of any relevant physological difference between strains.

VITA

Clark Jett

Candidate for the Degree of

Master of Science

Thesis: STRUCTURE FUNCTION STUDIES OF THE NDHD4 PROTEIN OF THE CO_2 UPTAKE MECHANISM IN *SYNECHOCOCCUS ELONGATUS* sp. PCC 7942

Major Field: Microbiology, Cell And Molecular Biology

Biographical:

Education:

Completed the requirements for the Master of Science in Microbiology, Cell and Molecular Biology at Oklahoma State University, Stillwater, Oklahoma in July, 2022.

Completed the requirements for the Bachelor of Science in Biology at University of Wyoming, Laramie, Wyoming in 2019.

Experience:

Graduate Research Assistnant at Oklahoma State University
Graduate Teaching Assistant at Oklahoma State University